



PERGAMON

Journal of Quantitative Spectroscopy &
Radiative Transfer 82 (2003) 5–44

Journal of
Quantitative
Spectroscopy &
Radiative
Transfer

www.elsevier.com/locate/jqsrt

The HITRAN molecular spectroscopic database: edition of 2000 including updates through 2001

L.S. Rothman^{a,*}, A. Barbe^b, D. Chris Benner^c, L.R. Brown^d, C. Camy-Peyret^e,
M.R. Carleer^f, K. Chance^a, C. Clerbaux^{f,g}, V. Dana^e, V.M. Devi^c, A. Fayt^h,
J.-M. Flaudⁱ, R.R. Gamache^j, A. Goldman^k, D. Jacquemart^a, K.W. Jucks^a,
W.J. Lafferty^l, J.-Y. Mandin^e, S.T. Massie^m, V. Nemtchinovⁿ, D.A. Newnham^o,
A. Perrinⁱ, C.P. Rinsland^p, J. Schroeder^q, K.M. Smith^o, M.A.H. Smith^p, K. Tang^q,
R.A. Toth^d, J. Vander Auwera^f, P. Varanasiⁿ, K. Yoshino^a

^aHarvard-Smithsonian Center for Astrophysics, Atomic and Molecular Physics Division, Cambridge, MA 02138, USA

^bGroupe de Spectrométrie Moléculaire et Atmosphérique, Université de Reims-Champagne-Ardenne,
51062 Reims, France

^cDepartment of Physics, The College of William and Mary, Williamsburg, VA 23187-8795, USA

^dJet Propulsion Laboratory, California Institute of Technology, Pasadena, CA 91109, USA

^eLaboratoire de Physique Moléculaire et Applications, Université Pierre et Marie Curie, 75252 Paris, France

^fLaboratoire de Chimie Physique Moléculaire, Université Libre de Bruxelles, B-1050 Brussels, Belgium

^gService d'Aéronomie, Université Pierre et Marie Curie, 75252 Paris, France

^hLaboratoire de Spectroscopie Moléculaire, Université Catholique de Louvain, B-1348 Louvain-la-Neuve, Belgium

ⁱLaboratoire de Photophysique Moléculaire, CNRS, Université Paris-Sud, Bât 350, 91405 Orsay, France

^jDepartment of Environmental, Earth and Atmospheric Sciences, Univ. of Mass Lowell, Lowell, MA 01854, USA

^kDepartment of Physics, University of Denver, Denver, CO 80208, USA

^lOptical Technology Division, NIST, Gaithersburg, MD 20899, USA

^mNational Center for Atmospheric Research, Boulder, CO 80307, USA

ⁿState University of New York at Stony Brook, Stony Brook, NY 11794, USA

^oRutherford Appleton Laboratory, Chilton, Didcot, Oxon OX11 0QX, UK

^pAtmospheric Sciences, NASA Langley Research Center, Hampton, VA 23681, USA

^qOntar Corp, 9 Village Way, North Andover, MA 01845-2000, USA

Received 26 February 2003; accepted 18 March 2003

Abstract

This paper describes the status circa 2001, of the HITRAN compilation that comprises the public edition available through 2001. The HITRAN compilation consists of several components useful for radiative transfer

*Corresponding author. Tel.: +1-617-49-57474; fax: +1-617-49-67519.

E-mail address: lrothman@cfa.harvard.edu (L.S. Rothman).

calculation codes: high-resolution spectroscopic parameters of molecules in the gas phase, absorption cross-sections for molecules with very dense spectral features, aerosol refractive indices, ultraviolet line-by-line parameters and absorption cross-sections, and associated database management software. The line-by-line portion of the database contains spectroscopic parameters for 38 molecules and their isotopologues and isotopomers suitable for calculating atmospheric transmission and radiance properties. Many more molecular species are presented in the infrared cross-section data than in the previous edition, especially the chlorofluorocarbons and their replacement gases. There is now sufficient representation so that quasi-quantitative simulations can be obtained with the standard radiance codes.

In addition to the description and justification of new or modified data that have been incorporated since the last edition of HITRAN (1996), future modifications are indicated for cases considered to have a significant impact on remote-sensing experiments.

© 2003 Elsevier Ltd. All rights reserved.

Keywords: HITRAN; Spectroscopic database; Molecular spectroscopy; Molecular absorption; Absorption cross-sections; Aerosol refractive indices

1. Introduction

This article describes the data and software that have been added, modified, or enhanced in the HITRAN (**H**igh Resolution **T**ransmission) compilation since the previous edition of 1996 [1]. The HITRAN molecular spectroscopic database and its associated components are similar in scope to the previous edition. An archival compilation was made available in late 2000 on an anonymous ftp-site (hereafter called HITRAN2k). Some major corrections and updates have also been posted on the regular HITRAN web-site (<http://cfa-www.harvard.edu/HITRAN>). This article traces these data sets through the end of 2001. Section 2 describes the changes for each molecule in the line-by-line portion of the compilation (historically referred to as the HITRAN database). This part of the article is key to understanding the basis for data improvements. Section 3 covers a rapidly expanding portion of the compilation, the infrared cross-sections. Section 4 describes the ultraviolet data sets, both line-by-line and cross-sections. Section 5 summarizes the tables of indices of refraction for various sets of aerosols. Section 6 describes the associated software that accompanies the compilation.

The file structure of the compilation is shown in Fig. 1. The compilation as a whole is called HITRAN Atmospheric Workstation (HAWKS).

2. Discrete molecular transitions: the HITRAN database

The line-by-line portion of the compilation contains fundamental spectroscopic parameters for their most abundant isotopologues of a number of molecules. The parameters of each spectral line or transition (equivalent to a record in the database) are given in Table 1. As adopted since the edition [2] of 1986, the total length of the record is 100 bytes composed of 16 fields. In future editions, the number of parameters will be increased, and the record length will be 160 bytes. It should be noted that the parameters are independent quantities, valuable as input to various computer codes that simulate transmittance or radiance in gaseous media. They have been chosen according to internationally

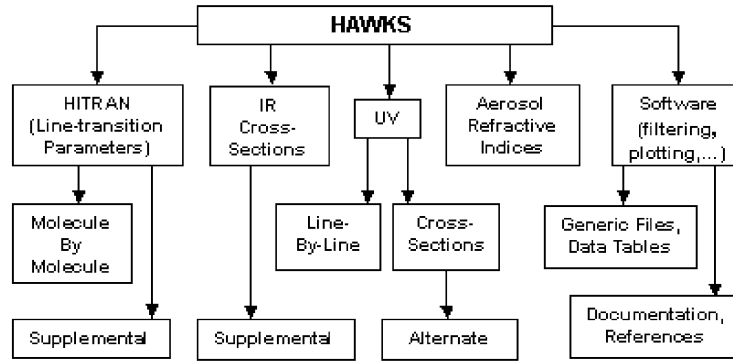


Fig. 1. File structure of HAWKS compilation.

Table 1
Format for HITRAN line transitions

Parameter	Symbol definition	Field length	Type	Comments
N	Molecule number	2	Integer	HITRAN chronological assignment
I	Isotopologue/isotopomer number	1	Integer	Ordering by terrestrial abundance
ν	Vacuum wavenumber	12	Real	In cm^{-1}
S	Intensity	10	Real	In $\text{cm}^{-1}/(\text{molecule cm}^{-2})$ at standard 296 K
R	Weighted transition-moment squared	10	Real	In Debye ² (to be changed to Einstein-A coefficient in future)
γ_{air}	Air-broadening half-width	5	Real	HWHM at 296 K (in $\text{cm}^{-1} \text{atm}^{-1}$) (Lorentzian half-width)
γ_{self}	Self-broadening half-width	5	Real	HWHM at 296 K (in $\text{cm}^{-1} \text{atm}^{-1}$) (Lorentzian half-width)
E''	Lower-state energy	10	Real	In cm^{-1}
n	Temperature dependence	4	Real	Temperature-dependent exponent for γ_{air}
δ	Air-pressure shift	8	Real	In $\text{cm}^{-1} \text{atm}^{-1}$
ν'	Upper-state "global" quanta index	3	Integer	See Table 3
ν''	Lower-state "global" quanta index	3	Integer	See Table 3
Q'	Upper-state "local" quanta	9	Hollerith	See Table 4
Q''	Lower-state "local" quanta	9	Hollerith	See Table 4
I_{err}	Uncertainty indices	3	Integer	Accuracy of 3 critical parameters (ν , S , and γ_{air})
I_{ref}	Reference indices	6	Integer	References for 3 critical parameters (ν , S , and γ_{air})

Note: For the intensity and weighted square of the transition moment, scientific notation is used, e.g., the type in FORTRAN is E10.3.

accepted modeling schemes. Necessary quantities that are more general in scope, such as the partition sum or the isotopic abundance, for example, are contained in associated tables in the compilation. A detailed summary of the definitions and the use of the parameters is given in Appendix A of Ref. [1].

The molecules present in HITRAN are shown in Table 2. The molecule numbers reflect the chronological entry into HITRAN. Historically, HITRAN has dealt with absorbers in the terrestrial atmosphere whose absorption properties contributed to measurable transmission or emission in remote-sensing experiments. The number of transitions included in the database is limited by: (1) a reasonable minimum cutoff in absorption intensity, (2) lack of sufficient experimental data, or (3) lack of calculated transitions. The strong dipole moments of some of the molecules have necessitated the inclusion of several isotopologues, as seen in the third column of Table 2, using the old Air Force Geophysics Laboratory (AFGL) shorthand notation for isotopologues (for example, 626 for $^{16}\text{O}^{12}\text{C}^{16}\text{O}$ and 636 for $^{16}\text{O}^{13}\text{C}^{16}\text{O}$) and isotopomers (for example 668 for $^{16}\text{O}^{16}\text{O}^{18}\text{O}$ and 686 for $^{16}\text{O}^{18}\text{O}^{16}\text{O}$). The fourth column gives the fractional abundance of the isotopologue as adopted in the HITRAN database, derived from De Bievre et al. [3]. The fifth column of Table 2 gives the overall spectral coverage rounded down for the lower wavenumber and up for the upper end of the range. For some molecules the intensity cutoff has been lowered in order to account for sequences of very high vibrational transitions that impact non-local thermodynamic equilibrium (NLTE) simulations; this is the case for both NO and OH, with resultant increases in their spectral coverage.

The molecules for which data are included in HITRAN are mostly composed of small numbers of atoms and low total molecular weight. Large polyatomic molecules have many normal modes of vibration and “heavy” species have fundamentals at very low wavenumbers. For two of the molecules in HITRAN, SF_6 and ClONO_2 , we have put the parameters for this edition in a supplemental folder (see Fig. 1). The rationale for this is that the line-by-line parameters only represent a few bands, and neglect many significant hot bands for the “heavy” species. In fact, the ν_9 vibrational (torsional) fundamental of ClONO_2 is below the nominal value of kT/hc of the atmosphere (about 200 cm^{-1}), where k , h , and c are the Boltzmann constant, Planck’s constant, and the speed of light (in vacuum), respectively. For most applications, the IR cross-sections of these molecules in HAWKS provide a better simulation.

In HITRAN, as shown in Table 1, the line transition has been given with upper and lower “global” quanta, and also upper and lower “local” quanta. The global quanta have been organized into 10 classes, and are shown in Table 3. The local quanta have been classified into six groups, as shown in Table 4.

The uncertainty indices that are used in HITRAN are defined in Table 5. This table also includes definitions for three more uncertainty indices that will be used in the next HITRAN edition.

Table 6 summarizes the range of values of parameters in HITRAN of air- (γ_{air}) and self-broadened (γ_{self}) half-widths, temperature dependence of air-broadened width (n), and air-pressure shift (δ). This table is meant as a rough guide. The extrema are for all bands of all of the isotopologues of a molecule; hence, if values exist only for one band, those will be indicated in the table. This table is useful in estimating unknown parameters, but particular caution should be used for estimating pressure-shift parameters, where values are slowly appearing in HITRAN, often just for a few bands.

The following sub-sections cover those molecules whose parameters have been updated since the last edition of HITRAN. The descriptions are generally by band regions. Future improvements are also mentioned where necessary.

2.1. H_2O (molecule 1)

Updates to two separate spectral regions for the water–vapor parameters in HITRAN were made since the last edition.

Table 2
Summary of isotopologues represented in HITRAN

Number	Molecule	Isotopologue (AFGL notation) ^a	Fractional abundance	Spectral coverage (cm ⁻¹)	Number of lines
1	H ₂ O	161	0.997317	0–22657	31683
		181	0.00199983	6–13901	7424
		171	0.000372	6–11144	3755
		162	0.00031069	0–5508	9796
		182	0.000000623	1173–1685	438
		172	0.000000116	1234–1599	175
2	CO ₂	626	0.98420	442–9649	27123
		636	0.01106	497–8105	8836
		628	0.0039471	507–8133	13313
		627	0.000734	554–6962	6625
		638	0.00004434	567–4947	2312
		637	0.00000825	584–3642	1584
		828	0.0000039573	615–3670	721
		728	0.00000147	626–2359	288
3	O ₃	666	0.992901	0–4061	161281
		668	0.00398194	0–1178	19147
		686	0.00199097	1–1146	7513
		667	0.000740	0–821	58254
		676	0.000370	0–823	28938
4	N ₂ O	446	0.990333	0–5132	19037
		456	0.0036409	5–3463	2106
		546	0.0036409	4–3474	2161
		448	0.00198582	555–3464	2000
		447	0.000369	586–3483	871
5	CO	26	0.98654	3–8465	917
		36	0.01108	3–6279	780
		28	0.0019782	3–6267	760
		27	0.000368	3–6339	728
		38	0.00002222	3–6124	712
		37	0.00000413	1807–6197	580
6	CH ₄	211	0.98827	0–6185	147153
		311	0.01110	0–6070	28793
		212	0.00061575	7–3307	35519
7	O ₂	66	0.995262	0–15927	1430
		68	0.00399141	1–15852	671
		67	0.000742	0–14537	4186
8	NO	46	0.993974	0–3967	16288
		56	0.0036543	1609–2061	699
		48	0.00199312	1601–2039	679
9	SO ₂	626	0.94568	0–4093	38566
		646	0.04195	2463–2497	287
10	NO ₂	646	0.991616	0–3075	104224
11	NH ₃	4111	0.9958715	0–5295	27994
		5111	0.0036613	0–5180	1090
12	HNO ₃	146	0.989110	0–1770	171504
13	OH	61	0.997473	0–19268	39900
		81	0.00200014	0–7	65
		62	0.00015537	0–2	90

Table 2 (continued)

Number	Molecule	Isotopologue (AFGL notation) ^a	Fractional abundance	Spectral coverage (cm ⁻¹)	Number of lines
14	HF	19	0.99984425	41–11536	107
15	HCl	15	0.757587	20–13458	284
		17	0.242257	20–10995	249
16	HBr	19	0.50678	16–9759	651
		11	0.49306	16–9758	642
17	HI	17	0.99984425	12–8488	806
18	ClO	56	0.75591	0–1208	3599
		76	0.24172	0–1200	3631
19	OCS	622	0.93739	0–4119	10554
		624	0.04158	0–4116	4186
		632	0.01053	0–4013	2283
		623	0.007399	509–4116	1802
		822	0.001880	0–4042	1096
20	H ₂ CO	126	0.98624	0–2999	1772
		136	0.01108	0–73	563
		128	0.0019776	0–48	367
21	HOCl	165	0.75579	0–3800	8057
		167	0.24168	0–3800	7508
22	N ₂	44	0.9926874	1922–2626	120
23	HCN	124	0.98511	2–3422	703
		134	0.01107	2–98	34
		125	0.0036217	2–101	35
24	CH ₃ Cl	215	0.74894	679–3173	5311
		217	0.23949	674–3162	4044
25	H ₂ O ₂	1661	0.994952	0–1500	5444
26	C ₂ H ₂	1221	0.97760	604–3359	2879
		1231	0.02197	613–3375	236
27	C ₂ H ₆	1221	0.97699	720–3001	4749
28	PH ₃	1111	0.99953283	708–1411	2886
29	COF ₂	269	0.98654	725–1982	54866
30	SF ₆	29	0.95018	940–953	11520
31	H ₂ S	121	0.94988	2–4257	12330
		141	0.04214	5–4172	4894
		131	0.007498	5–4099	3564
32	HCOOH	126	0.983898	1060–1162	3388
33	HO ₂	166	0.995107	0–3676	38808
34	O	6	0.997628	68–159	2
35	ClONO ₂	5646	0.74957	763–798	21988
		7646	0.23970	765–791	21110
36	NO ⁺	46	0.993974	1634–2531	1206
37	HOBr	169	0.5056	0–316	2177
		161	0.4919	0–316	2179
38	C ₂ H ₄	221	0.9773	701–3243	12697
		231	0.02196	2947–3181	281

Note: SF₆ and ClONO₂ are relegated to the supplemental directory (see text).

^aThe majority of molecular entities in HITRAN are isotopologues, except for some isotopomers of ozone and nitrous oxide.

Table 3

Notation of global quanta identification for the 10 classes

Class definition for HITRAN molecules	Upper- and lower-state “global” quanta
Class 1: Diatomic molecules CO, HF, HCl, HBr, HI, N ₂ , NO ⁺	ν_1
Class 2: Diatomic molecules with different electronic levels O ₂	$X\nu_1$
Class 3: Diatomic molecules with Π -doublet electronic state NO, OH, ClO	$Xi\nu_1$
Class 4: Linear triatomic N ₂ O, OCS, HCN	$\nu_1\nu_2l_2\nu_3$
Class 5: Linear triatomic with large Fermi resonance CO ₂	$\nu_1\nu_2l_2\nu_3r$
Class 6: Non-linear triatomic H ₂ O, O ₃ , SO ₂ , NO ₂ , HOCl, H ₂ S, HO ₂ , HOBr	$\nu_1\nu_2\nu_3$
Class 7: Linear tetratomic C ₂ H ₂	$\nu_1\nu_2\nu_3\nu_4\nu_5l \pm r$
Class 8: Pyramidal tetratomic NH ₃ , PH ₃	$\nu_1\nu_2\nu_3\nu_4 S$
Class 9: Non-linear tetratomic H ₂ CO, H ₂ O ₂ , COF ₂	$\nu_1\nu_2\nu_3\nu_4\nu_5\nu_6$
Class 10: Pentatomic or greater polyatomic CH ₄ CH ₃ D, CH ₃ Cl, C ₂ H ₆ , HNO ₃ , SF ₆ , HCOOH, ClONO ₂ , C ₂ H ₄	$\nu_1\nu_2l_2\nu_3l_3\nu_4l_4l$ Explicit mode notation

Notes : This notation of the global quanta field will be the notation for the next HITRAN format (15 characters instead of 3). In the current HITRAN edition, the global quanta are represented by an index (format I3). The correspondence of these numbers and the local quanta can be found in the ftp site in the program bd.vibs.for. In the next edition of HITRAN, the local quanta of this table will be incorporated in the HITRAN format. ν_j is the quantum number associated with the normal mode of vibration j , l_j is the vibrational angular momentum quantum number associated with the degenerate bending mode j , and l is defined as the absolute value of the sum of the vibrational angular momentum quantum number l_j . For classes 2 and 3, X designates the electronic state of the molecule, and for class 3 i corresponds to either 1/2 or 3/2. For the notation of class 5, see Ref. [4]. For the notation of class 7, see Ref. [5]. For class 8, S is the symmetry of the level. For the notation of class 10, see Ref. [6].

Toth [7–9] completed an analysis of laboratory spectra, including isotopic species and hot bands, from 500 to 2820 cm⁻¹. Updates are for positions, intensities, air-broadening coefficients, self-broadening coefficients, and pressure-induced shifts [7–12]. Default values as a function of the running index m were used for the temperature-dependence coefficient of γ_{air} , n . For a few lines we have adopted the temperature dependence of widths from Remedios [13]; these lines are clearly identified using the reference index for air-broadened half-width. (In the next edition of HITRAN, three new indices will be added, namely for reference to the self-broadened half-width, the temperature dependence of the air-broadened half-width, and the pressure shift.) Data for two rare isotopologues, HD¹⁸O and HD¹⁷O, numbers 5 and 6 in the HITRAN ordering scheme by terrestrial abundance, are included in this update for the first time. However, many lines of the ν_1 band (100–000) of the principal isotopologue overlap the shortwave part of this region. The lines of the latter band remain the

Table 4

Formats (in FORTRAN) for the six groups of local quanta identification

Group classification and HITRAN molecules	Upper-state “local” quanta	Lower-state “local” quanta
Group 1: Asymmetric rotors ^a H ₂ O, O ₃ , SO ₂ , NO ₂ , HNO ₃ , H ₂ CO, HOCl, H ₂ O ₂ , COF ₂ , H ₂ S, HO ₂ , HCOOH, ClONO ₂ , HOBr, C ₂ H ₄	$J', K'_a, K'_c, F', \text{Sym}'$ I2, I2, I2, I2, A1	$J'', K''_a, K''_c, F'', \text{Sym}$ I2, I2, I2, I2, A1
Group 2a: Diatomic and linear molecules with integer J CO ₂ , N ₂ O, CO, HF, HCl, OCS, N ₂ , HCN, C ₂ H ₂ , NO ⁺	$_ , \text{Br}, F'' _$ 5X, A1, I2, 1X	$_ , \text{Br}, J'', \text{Sym}''$ 4X, A1, I3, A1
Group 2b: Diatomic and linear molecules with integer J , and half-integer F HBr, HI	$_ , \text{Br}, _ , F''$ 5X, A1, 1X, F4.1	$_ , \text{Br}, J'', \text{Sym}$ 2X, A1, I3, A1
Group 3a: Spherical rotors SF ₆	$J', R', C', N', _$ I2, I2, A2, I2, 1X	J'', R'', C'', N'' I2, I2, A2, I2, 1X
Group 3b: Spherical rotors CH ₄ (not CH ₃ D)	$J', C', \alpha', _$ I2, A2, I3, 2X	$J'', C'', \alpha'', _$ I2, A2, I3, 2X
Group 4a: Symmetric rotors CH ₃ D	$J', K', _ , C', _$ I2, I2, 2X, A2, 1X	$J'', K'', _ , C'', _$ I2, I2, 2X, A2, 1X
Group 4b: Symmetric rotors CH ₃ Cl, C ₂ H ₆ , PH ₃	$J', K', C', _ , \text{Sym}'$ I2, I2, A2, 2X, A1	$J'', K'', C'', _ , \text{Sym}''$ I2, I2, A2, 2X, A1
Group 4c: Symmetric rotors NH ₃	$J', K', l', _ , \text{Sym}'$ I2, I2, I2, 2X, A1	$J'', K'', l'', _ , \text{Sym}''$ I2, I2, I2, 2X, A1
Group 5: Triplet- Σ ground electronic states O ₂	$_ , \text{Br}, F'' , _$ 3X, A1, F4:1, 1X	$\text{Br}, N'' , \text{Br}, J'' , _ , \text{Sym}''$ A1, I2, A1, I2, 2X, $_ ,$ A1
Group 6a: Doublet- Π ground electronic states ^b (half-integer J , integer F) OH, ClO	$_ , \text{Br}, F'' , _$ 5X, A1, I2, 1X	$_ , \text{Br}, J'' , \text{Sym}''$ 3X, A1, F4:1, A1
Group 6b: Doublet- Π ground electronic states (half-integer J , half-integer F) NO	$_ , F' , _ , F''$ 2X, F4:1, 1X, F4:1	$_ , \text{Br}, J'' , \text{Sym}''$ 1X, A1, F4:1, A1

Notes: Prime and double primes refer to upper and lower states, respectively; Br is the O-, P-, Q-, R-, or S-branch symbol; J is the quantum number associated with the total angular momentum excluding nuclear spin; F is the quantum number associated with the total angular momentum including nuclear spin (when necessary for a few transitions). In group 3a, R is the quantum number associated with the nuclear orbital angular momentum and N is the quantum number associated with the rotational angular momentum. The quantum notation C and α is described in Ref. [6]. N is the total angular momentum including spin and rotation for O₂. Sym is e or f for l -type doubling, + or – for required symmetry symbols, and d or q for magnetic-dipole or electric-quadrupole transitions (for O₂ and N₂).

^aFor NO₂, $F - J$ has been used instead of F .

^bFor OH, the format of branch (Br) in the lower-state quanta field is 2A1 to accommodate the total orbital angular momentum N as well as J . Notice that the format for NO, HBr, and HI have 11 bytes in the upper-quanta field, and 7 bytes in the lower-quanta field, instead of 9 bytes and 9 bytes as indicated in Table 1.

Table 5
Uncertainty codes adopted for HITRAN

Line position and air-pressure shift (cm^{-1})		Intensity, half-width (air and self) and temperature dependence of half-width	
Code	Uncertainty range	Code	Uncertainty range
0	≥ 1.0 or Unreported	0	Unreported or unavailable
1	≥ 0.1 and < 1.0	1	Default or constant
2	≥ 0.01 and < 0.1	2	Average or estimate
3	≥ 0.001 and < 0.01	3	$\geq 20\%$
4	≥ 0.0001 and < 0.001	4	$\geq 10\%$ and $< 20\%$
5	≥ 0.00001 and < 0.0001	5	$\geq 5\%$ and $< 10\%$
6	< 0.00001	6	$\geq 2\%$ and $< 5\%$
		7	$\geq 1\%$ and $< 2\%$
		8	$< 1\%$

same as in the earlier editions of HITRAN. It should be remarked here that the data of Toth [7] did not include the fundamental of HDO, and an update was required to HITRAN2k.

Dramatic improvements of atmospheric retrievals have been demonstrated using the update to HITRAN in this region [14,15].

The intensities of all lines in HITRAN beyond 8000 cm^{-1} have been adjusted. This was due to the correction of a problem with intensity unit conversion of lines in the near-IR and visible found by Giver et al. [16]. A major update has occurred within this broad region, namely with the addition of the 3ν polyad of bands from 9600 to 11400 cm^{-1} . The positions and intensities come from the observations and analysis by Brown et al. [17]. Positions for about 100 lines in this region, however, come from the earlier work of Chevillard et al. [18]. For the second isotopologue, H_2^{18}O , the calculated positions predicted by Partridge and Schwenke [19] have occasionally been superseded using observed upper levels from Chevillard et al. [20]. Observed intensities [20] were used to scale the calculations of Ref. [19]. The few lines of the third isotopologue, H_2^{17}O , that survive the HITRAN intensity cutoff in this region have line positions and intensities taken from Camy-Peyret et al. [21].

Air-broadened half-widths for all bands in the 9600 to 11400 cm^{-1} region come from Brown et al. [17], but in some cases are the result of averaging over many bands. Self-broadened widths for B-type bands are derived from Ref. [17]; self-broadened widths for A-type bands come from unpublished results of Toth. For unassigned lines we use a default value $0.444 \text{ cm}^{-1} \text{ atm}^{-1}$ for γ_{self} . The temperature dependence of the air-broadened half-width, n , is either a function of a running index m (equal to $-J$, J , or $J+1$, for the P-, Q-, and R-branches, respectively), values adopted from other bands, or is set to a value of 0.68 for unassigned lines. It should be recalled from the previous editions of HITRAN that there still exist numerous unassigned lines of water vapor in the visible region in HITRAN. These lines come from direct experiment at 296 K, and are flagged by a minus one (-1) in the field for lower-state energy. Finally, the air-induced pressure shift, δ , has been set to either $-0.0111 \text{ cm}^{-1} \text{ atm}^{-1}$ or determined from an average of many bands [17].

There are works in progress that will significantly update the water-vapor parameters in the next edition of HITRAN. Among these are the evaluations of long-path laboratory observations in the

Table 6

Range of parameters in HITRAN for air- (γ_{air}) and self-broadened (γ_{self}) half-widths, temperature dependence of air-broadened width (n), and air-pressure shift (δ)

	Molecule	γ_{air}		γ_{self}		n		δ	
		Min.	Max.	Min.	Max.	Min.	Max.	Min.	Max.
1.	H ₂ O	0.0023	0.1099	0.0	0.7048	0.28	0.97	-0.0312	0.0212
2.	CO ₂	0.0554	0.0949	0.0523	0.1279	0.49	0.78	-0.00372	0.0
3.	O ₃	0.0494	0.0836	0.0809	0.1119	— 0.76 —		— 0.0 —	
4.	N ₂ O	0.0686	0.0974	0.0	0.127	0.64	0.82	— 0.0 —	
5.	CO	0.04	0.0789	0.046	0.0878	— 0.69 —		— 0.0 —	
6.	CH ₄	0.0000	0.0987	0.0137	0.2045	0.1300	1.07	-0.03276	0.01797
7.	O ₂	0.0279	0.0601	0.0274	0.0654	0.63	0.74	-0.009	0.0
8.	NO	0.041	0.0687	0.0	0.076	0.5	0.71	-0.004	0.0
9.	SO ₂	0.1	0.152	0.0	0.4	0.5	0.75	— 0.0 —	
10.	NO ₂	0.0631	0.0841	— 0.095 —		— 0.97 —		— 0.0 —	
11.	NH ₃	0.0531	0.11	0.0585	0.6603	0.45	0.95	— 0.0 —	
12.	HNO ₃	— 0.11 —		0.0	0.73	— 0.75 —		— 0.0 —	
13.	OH	0.04	0.095	— 0.0 —		0.5	0.66	— 0.0 —	
14.	HF	0.01	0.105	0.0	0.7295	0.22	1.	-0.029	0.012
15.	HCl	0.005	0.0984	0.0221	0.264	0.05	0.76	-0.0129	0.001
16.	HBr	0.015	0.123	0.05	0.1378	— 0.5 —		— 0.0 —	
17.	HI	— 0.05 —		0.01	0.12	— 0.5 —		— 0.0 —	
18.	ClO	0.085	0.093	— 0.0 —		0.5	0.75	— 0.0 —	
19.	OCS	0.07	0.1092	0.0	0.1685	0.3	0.9	— 0.0 —	
20.	H ₂ CO	0.107	0.108	— 0.0 —		— 0.5 —		— 0.0 —	
21.	HOCl	— 0.06 —		— 0.0 —		— 0.5 —		— 0.0 —	
22.	N ₂	0.0314	0.053	0.0314	0.053	— 0.5 —		— 0.0 —	
23.	HCN	0.0819	0.1566	— 0.0 —		— 0.5 —		— 0.0 —	
24.	CH ₃ Cl	0.08	0.1238	— 0.0 —		— 0.5 —		— 0.0 —	
25.	H ₂ O ₂	— 0.1 —		— 0.0 —		— 0.5 —		— 0.0 —	
26.	C ₂ H ₂	0.04	0.1158	0.0812	0.1969	— 0.75 —		-0.001	0.0
27.	C ₂ H ₆	— 0.1 —		— 0.0 —		— 0.5 —		— 0.0 —	
28.	PH ₃	— 0.075 —		— 0.0 —		— 0.5 —		— 0.0 —	
29.	COF ₂	— 0.0845 —		— 0.175 —		— 0.94 —		— 0.0 —	
30.	SF ₆	— 0.05 —		— 0.08 —		— 0.65 —		— 0.0 —	
31.	H ₂ S	0.08	0.15	— 0.17 —		— 0.75 —		— 0.0 —	
32.	HCOOH	— 0.1 —		— 0.0 —		— 0.75 —		— 0.0 —	
33.	HO ₂	— 0.107 —		— 0.0 —		0.5	0.67	— 0.0 —	
34.	O	— Not Applicable —							
35.	ClONO ₂	— 0.14 —		— 0.8 —		— 0.5 —		— 0.0 —	
36.	NO ⁺	— 0.06 —		— 0.0 —		— 0.5 —		— 0.0 —	
37.	HOBr	— 0.06 —		— 0.0 —		— 0.67 —		— 0.0 —	
38.	C ₂ H ₄	— 0.087 —		— 0.09 —		— 0.82 —		— 0.0 —	

Note: A “zero” as value can signify no value given; ranges indicate extremes for some bands, other bands may be defaults or blank.

short-wave region [22–26]. It is expected that these studies, as well as an analysis [27] to identify isotopic lines that may be incorrectly assigned in the literature, will greatly improve this region for many applications. In addition, there are a dozen lines in this region that are apparently duplicates, that is, they have identical quantum assignments but different line positions. Ten lines also have rotational assignments even though the upper-state vibration is listed as unknown. About 20 lines have quantum assignments for the transition, yet the lower-state energy is listed as -1 (the HITRAN convention for unidentified quanta). These problems have existed for H_2O in the past, but over time the editions of HITRAN have had a considerable reduction in these inconsistencies.

Another significant improvement that is imminent is in the 1.3- to 1.5- μm region. In the current edition of HITRAN, the data were preliminary results of Toth, which later appeared in Ref. [28]. The results in the latter work [28] are a definite improvement, as shown by Lepère et al. [29] and by Parvite et al. [30].

New calculations of half-widths [31] will be considered for all transitions of water vapor throughout the database in the future.

2.2. CO_2 (molecule 2)

There are no updates for carbon dioxide spectral line parameters since the previous edition of HITRAN [1]. However, many improvements are planned for the next update. There are several deficiencies with the intensities of CO_2 bands in the database, especially in the 1- to 3- μm region. In the previous HITRAN database, there were only a few measurements of the weak CO_2 bands; the intensities of weak, unmeasured lines were calculated using the direct numerical diagonalization (DND) technique [32]. The results in the short-wave spectral region were limited somewhat by both the truncation of the energy matrix (yielding less accurate line positions) and by the method used to determine the relative intensities of the P- and R-branches (Herman–Wallis factors). There have been numerous high-resolution intensity measurements that need to be incorporated into HITRAN. Among them are the measurements of Devi et al. [33], Giver et al. [34], Goldman et al. [35], and Henningsen and Simonsen [36].

Many of the positions and intensities of CO_2 lines in the HITRAN database are currently inaccessible to laboratory measurement. There are two promising methods for the calculation of energy levels and intensities of CO_2 lines. The variational method, similar to DND, has been successfully pursued by Aguir et al. [37]. The method of effective operators, advanced by Tashkun et al. [38], has produced a database in HITRAN format.

2.3. O_3 (molecule 3)

The ozone parameters have remained the same since the last edition. Many improvements, enhancements, and extensions in spectral coverage will soon be available. A comprehensive review of the status for ozone is described in this issue by Rinsland et al. [39].

2.4. N_2O (molecule 4)

The R(3) line of the ν_2 fundamental of the principal isotope of nitrous oxide, $^{14}\text{N}_2^{16}\text{O}$, which was inadvertently omitted from the previous edition, has been restored; this problem was noted

in the previous article [1]. Numerous improvements for nitrous oxide line parameters have been achieved, but were not completed in time for the edition of HITRAN described in this paper. Among the improvements will be an update in the 17- μm region, and the replacement of data for two weak bands in the 10- μm region, (00⁰1–10⁰0) and (02²0–00⁰0), that have poorly determined intensities in HITRAN. The data in the 17- μm region come from Johns et al. [40], while the results for the two bands in the 10- μm region come from Daumont et al. [41]. Furthermore, Toth [42] measured line positions and intensities in the range from 3515 to 7800 cm^{-1} and Daumont et al. [43] measured more than 3000 line intensities in 66 bands in the 3788–5319- cm^{-1} region. A line list in HITRAN format covering the latter spectral range is currently being prepared.

2.5. CO (molecule 5)

No changes for carbon monoxide have been made since the previous edition of HITRAN. For the second overtone of $^{12}\text{C}^{16}\text{O}$ around 1.6 μm , different groups [44–47] have come to the conclusion that the intensity values in HITRAN are overestimated by 5–7%. Similarly, for the first overtone near 2.4 μm , two recent studies [48,49] indicate that the HITRAN intensities are 1–6% larger than the measured values. The current HITRAN air-broadening coefficients agree with recent laboratory measurements [47,48,50] in the fundamental and first two overtones within $\pm 2\%$ for transitions with $3 < |m| < 19$. Outside this range, the HITRAN air-broadening coefficients are 3–10% smaller than the measured values. The temperature dependence exponent for air-broadening is a constant value of 0.69 $\text{cm}^{-1} \text{atm}^{-1}$ for all CO transitions in HITRAN2k. However, a recent laboratory study in the 1–0 and 2–0 bands [48] indicates that the temperature exponents are closer to 0.75 for low- J transitions, and there is a significant $|m|$ -dependence. This same study reports measured air-induced line shift coefficients averaging $-0.003 \text{ cm}^{-1} \text{atm}^{-1}$ in the 1–0 band and ranging from -0.003 to $-0.007 \text{ cm}^{-1} \text{atm}^{-1}$ in the 2–0 band. Another study [47] reports air shifts between -0.003 and $-0.009 \text{ cm}^{-1} \text{atm}^{-1}$ in the 3–0 band. However, the air-shift coefficients remain set to zero in HITRAN2k. The HITRAN2k self-broadening coefficients and recent measurements [44–55] all agree within $\pm 5\%$. With one exception [53], all the broadening and shift measurements cited above are for the main isotopologue $^{12}\text{C}^{16}\text{O}$. According to two recent studies [53,56], the self-broadening coefficients of the lines of $^{13}\text{C}^{16}\text{O}$ are apparently smaller by 2% [53] than those of the corresponding lines of $^{12}\text{C}^{16}\text{O}$, while the N_2 -broadening coefficients of the lines of $^{13}\text{C}^{16}\text{O}$ are 5–7% smaller [56] than the corresponding $^{12}\text{C}^{16}\text{O}$ values. However, adoption of the apparent differences in the parameters of the two isotopologues should be based upon more measurements that confirm this fact, before they are considered for inclusion in a future edition of HITRAN.

2.6. CH₄ (molecule 6)

Methane in the HITRAN database comprises line parameters for three isotopologues, $^{12}\text{CH}_4$, $^{13}\text{CH}_4$, and $^{12}\text{CH}_3\text{D}$ and covers the spectral region from 0 to 6185 cm^{-1} . A major update has been accomplished for methane from 500 to 5500 cm^{-1} . This update was completed after the HITRAN2k edition, and became available in 2001. Regions below 500 cm^{-1} and above 5500 cm^{-1} retain lines from the previous database [1].

The status and description of methane line parameters in HITRAN, as well as ongoing progress, are described by Brown et al. [6] in this issue. The number of lines of methane has increased dramatically (from 48 032 to 211 465 lines) with the HITRAN 2001 update, partly due to a lower intensity cutoff. Some minor caveats should be mentioned. The HITRAN convention for unassigned lines is to put a minus one (−1) as a flag in the lower-state energy field. However, for methane there are many unassigned lines with estimated values given for the lower-state energy. Most of these lines in question are above 5500 cm^{-1} . Two lines (3354.842341 and $3364.857096\text{ cm}^{-1}$) were not correctly sorted in wavenumber [57] (they were placed just after $3375.437932\text{ cm}^{-1}$). The intensity of a line located at $4576.668325\text{ cm}^{-1}$ has been mistakenly listed as negative [58]. These minor errors will be corrected in the next edition of HITRAN.

The notation for the methane quanta has been more standardized in the HITRAN 2001 update, as described in Ref. [6]. Table 4 shows the notation of the rotational quanta (groups 3b and 4a). Fig. 2 illustrates the change in coverage for methane between the current and previous editions of HITRAN. The stick plot was made with the HAWKS software (described in Section 6) that also indicates the dynamic range improvement. In general, when there is a high density of lines in the spectral interval, the plot displayed will have blue and red lines. This is to indicate the minimum and maximum value in each unresolved plotting element; expanding the x -axis scale will eliminate this overlap unless there are truly lines at the same wavenumber.

2.7. O_2 (molecule 7)

Two major updates were accomplished for oxygen since the last edition of HITRAN.

The line intensities in the $1.27\text{-}\mu\text{m}$ region, corresponding to transitions between the ground electronic state $X^3\Sigma_g^-$ and the electronic state $a^1\Delta_g$, were previously based upon very sparse measurements of the band. There have been more recent high-resolution laboratory measurements performed on this band. In the HITRAN 2001 update, line intensities for the principal isotopologue have been revised based upon the work of Lafferty and co-workers [59]. The results of Ref. [59] have been corroborated in another recent study by Smith and Newnham [60].

The atmospheric A band, between the ground electronic state $X^3\Sigma_g^-$ (with vibrational level $v=0$) and the electronic state $b^1\Sigma_g^-$ (with vibrational level $v=0$), centered at $0.76\text{ }\mu\text{m}$, has been revised in the present edition of HITRAN with the new measurements of Brown and Plymate [61]. However, in the line list, the positions of two lines located at 13161.6135 and $13161.6127\text{ cm}^{-1}$ are reversed [57].

The isotopic abundance factor had been inadvertently omitted from the line intensities in the $X^3\Sigma_g^-(v=0) \leftarrow X^3\Sigma_g^-(v=0)$ band (submillimeter region) of the $^{16}\text{O}^{17}\text{O}$ species. This error has been rectified in the current edition of HITRAN.

2.8. NO (molecule 8)

The line positions and intensities for the first overtone (2–0) and hot band (3–1) of nitric oxide have been updated, resulting from the work of Mandin et al. [62,63]. Additional parameters for the forbidden subbands of the first overtone have been updated from the work of Gillis and Goldman [64], which also provided the parameters for hot bands in this region.

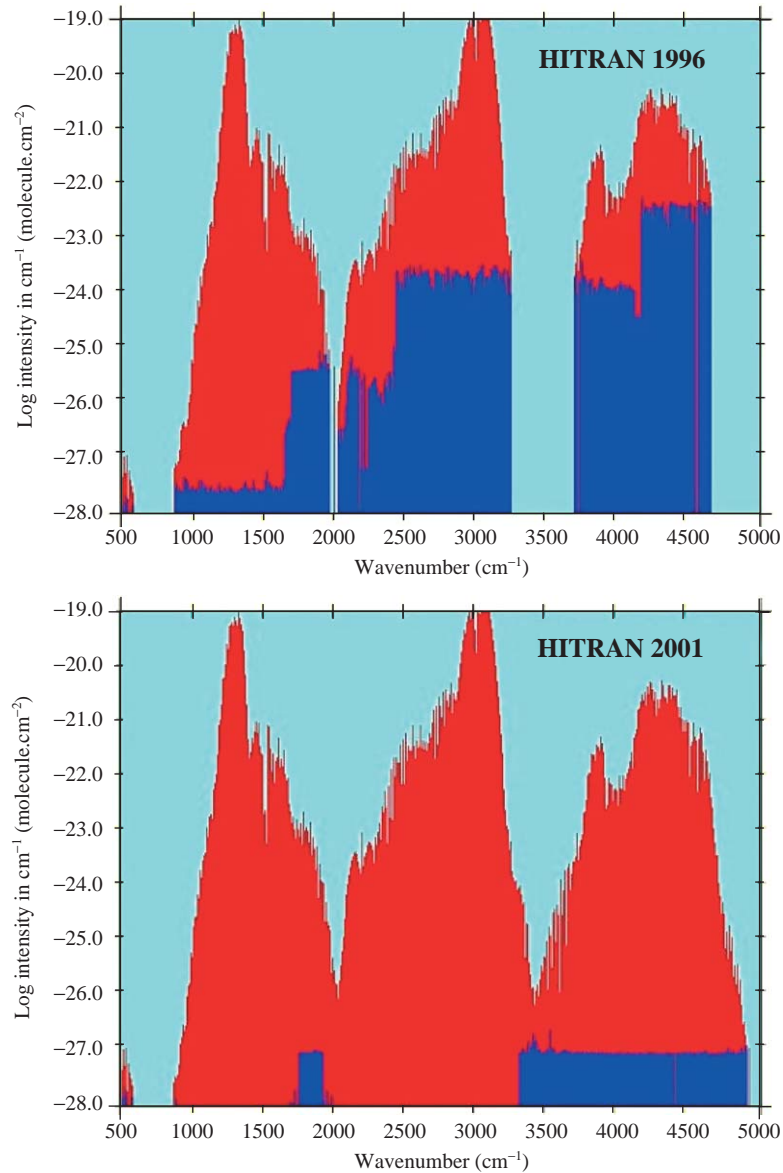


Fig. 2. Stick plots of the line intensities of methane in the previous and current editions of HITRAN. Blue and red lines are minimum and maximum intensities when lines are within the wavenumber scale of the plot (see text).

The air-broadened half-widths have been updated. For the (2–0) transitions, an algorithm based on Refs. [65,66] has been used. It was assumed that the validity of this algorithm applied for all $\Delta v = 2$ transitions including forbidden sub-bands. For the fundamental band of $^{14}\text{N}^{16}\text{O}$ and the allowed hot band (2–1), air-broadened half-widths have been adopted from the work of Chackerian et al. [67], which is also the source for the pressure shifts of parameters for all the NO infrared bands in HITRAN.

2.9. SO_2 (molecule 9)

No changes in sulfur dioxide line parameters have been made since the previous edition of HITRAN [1].

2.10. NO_2 (molecule 10)

A major update of the 3.4- μm region of nitrogen dioxide has been made, as recommended in the last article [1]. The update, which was made in 2001, replaces the spectral line parameters for the combination bands, (120–000) and (101–000), and the hot band (111–010). The line positions and intensities are taken from the work of Mandin et al. [68].

There has been a complete update of air-broadened half-widths and their temperature dependences, n , for the entire line list of NO_2 . For the air-broadened half-widths, an algorithm with a functional dependence on rotational quanta was adapted from the work of Dana et al. [69]. A mean value of the temperature dependence was adopted from the works of Devi et al. [70] and May and Webster [71]. A mean value has been adopted for the self-broadened half-width throughout the linelist from Perrin et al. [72]; previously there were no values given for this parameter for NO_2 in HITRAN. Fig. 3 illustrates the broad change in coverage for nitrogen dioxide between the current and previous editions of HITRAN.

2.11. NH_3 (molecule 11)

Improvements for ammonia incorporated into HITRAN2k are described in the article by Kleiner et al. [73] in this special issue. The update involved replacing pure-rotational and infrared transitions from 0 to 3700 cm^{-1} with new calculations for the $^{14}\text{NH}_3$ isotopologue, whereas in the 4000–5300 cm^{-1} region, parameters from the 1996 database were retained. Some transitions that were not fully identified were inappropriately assigned in the quanta fields. This is mentioned in Ref. [73] and should not cause serious problems.

2.12. HNO_3 (molecule 12)

An extensive update for nitric acid has been made in the 11- μm region. The two hot bands, $\nu_5 + \nu_9 - \nu_9$ and $3\nu_9 - \nu_9$, have been removed from the previous HITRAN and replaced by the hot band $\nu_5 + \nu_9 - \nu_9$ from Goldman et al. [74]. This replacement represents an update for both positions and intensities. The line intensities in this region may still be off as much as 8% due to missing hot bands [75]. A more accurate analysis of the 11- μm region using new laboratory high-resolution Fourier transform spectra is being performed, and is expected to improve positions and intensities for the next HITRAN edition [76].

The half-widths applied [77] are the same as used in previous editions of HITRAN [1,2].

2.13. OH (molecule 13)

Line parameters for all transitions of the principal isotopologue of the hydroxyl radical have been updated for this edition [78]. The new positions and intensities are the results of an improved

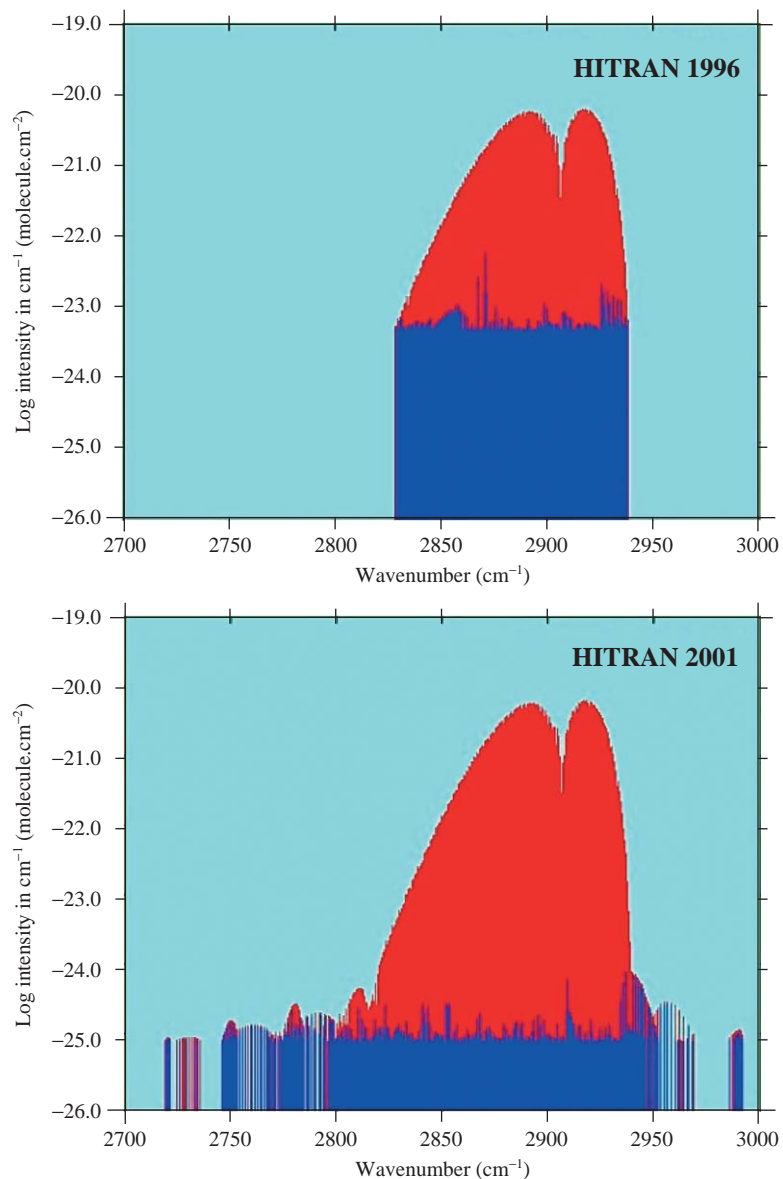


Fig. 3. Stick plots of the nitrogen dioxide line intensities in the previous and current editions of HITRAN. Blue and red lines are minimum and maximum intensities when lines are within the wavenumber scale of the plot (see text).

calculational method for the vibrational eigenfunctions. There are many overtone and hot bands included in HITRAN [1] because of interest in non-LTE applications with this molecule, and thus the usual terrestrial absorption cutoff for lines does not apply here. The new line parameters extend the transitions to cover $\Delta v = 0, \dots, 6$ with $v' = 0, \dots, 10$ and $J_{\max} = 49.5$, which significantly increases the number of lines in the database. Hyperfine structure (hfs) was not included in this new update;

hfs will be included in a future list and applies mainly to the $\Delta v=0$ transitions (the lesser abundant isotopologue lines that have been preserved from the previous editions do have hyperfine components listed).

2.14. HF (molecule 14)

No changes in hydrogen fluoride line parameters have been made since the previous edition of HITRAN [1].

2.15. HCl (molecule 15)

No changes in hydrogen chloride line parameters have been made since the previous edition of HITRAN [1].

2.16. HBr (molecule 16)

The pure-rotation lines and the fundamental band (1–0) for both isotopologues of hydrogen bromide have been updated. A detailed account of the improvements is given in [79].

2.17. HI (molecule 17)

Ref. [79] gives a comprehensive account of the improvements for the pure-rotation lines and fundamental band of hydrogen iodide made since the last edition of HITRAN.

2.18. ClO (molecule 18)

No changes in chlorine monoxide line parameters have been made since the previous edition of HITRAN [1].

2.19. OCS (molecule 19)

An extensive self-consistent IR line list computed by Fayt was used to update HITRAN from 490 to 4120 cm^{-1} . These parameters have been amalgamated with the pure-rotation bands already existing in HITRAN to form a complete set with many more bands than was previously catalogued. An additional isotopologue is now included in this list for the first time, namely $^{16}\text{O}^{12}\text{C}^{33}\text{S}$ (623 in AFGL code). In keeping with the HITRAN system of numbering isotopologues sequentially based on terrestrial abundances, the isotopologue $^{18}\text{O}^{12}\text{C}^{32}\text{S}$ (822) which had been labeled 4 in previous editions of HITRAN, has become number 5. The new line list represents a vast increase of bands in HITRAN that were not considered for previous editions of HITRAN: for the infrared domain, there are 10455 lines in 50 bands for the isotopologue 622, 4093 lines in 26 bands for 624, 2190 lines in 16 bands for 632, 1802 lines in 13 bands for 623, and 1012 lines in 10 bands for 822.

The calculated wavenumbers are based on the global analysis developed for this molecule [80–82]. The global analyses of the main isotopologues are regularly updated using new experimental data published in the literature. Since the 1991 global analysis [82], many quite accurate data have been introduced [83–98], giving a considerable improvement to the accuracy of the analyses. A statistical agreement is obtained with all available data. For the main isotopologue, the HITRAN data correspond to the 1998 global analysis [98]. For the other isotopic species, they correspond to the last published global analyses [86] noticeably improved by the introduction of experimental data from Refs. [90,96,97].

Recently, line positions for the two bands of the principal isotopologue at 1892 and 2062 cm^{-1} have been replaced by the sub-Doppler heterodyne frequency measurements of Mürtz et al. [99]. Interestingly, the line positions from Fayt et al. [80] for these bands generally agreed to within 10^{-6} cm^{-1} with the Mürtz et al. [99] fitted values, even though the HITRAN uncertainty criteria given for the former data was 5, that is, good to 10^{-5} cm^{-1} . Except for the highest J -lines of the 1892 band, the line position accuracy is now given as “6”, and these lines can be considered of frequency calibration quality.

Intensities are based on the work of Kagann [100] for the 500, 1650, and 4000- cm^{-1} regions, of Dang-Nhu et al. [101] for the 2575- cm^{-1} region, of Bouanich et al. [102] for the 850- cm^{-1} region, of Blanquet et al. [103] for the 1000- cm^{-1} region, and of Belafhal et al. [90,91] for the 1800- to 3200- cm^{-1} region. The intensities for the 2500- to 3100- cm^{-1} region [90] have been recalibrated according to more accurate measurements performed by Errera et al. [104]. Some intensities from Ref. [90] have been estimated by Brown [105] using a few spectra recorded with the Fourier transform spectrometer at Kitt Peak National Observatory. The intensities of the $\nu_1 + 2\nu_2$ band near 1900 cm^{-1} have been multiplied by a factor 1.22, those of the ν_3 band near 2000 cm^{-1} by 0.88, and those of the $4\nu_2$ band near 2100 cm^{-1} by 1.10. The validity of the applied corrections for $\nu_1 + 2\nu_2$ and $4\nu_2$ has been confirmed in the study of $^{18}\text{O}^{12}\text{C}^{32}\text{S}$ [96], whereas the original value for the ν_3 band was confirmed. Recent high-resolution observations at the University of Reims [106] in the 3- to 5- μm region have shown some discrepancies with values listed in the HITRAN database. A mean difference of more than 12% has been observed in the intensities of the ν_3 band of the main isotopologue compared to HITRAN2k. Further validations are ongoing. The listed intensities of the $2\nu_3$ band of $^{16}\text{O}^{12}\text{C}^{32}\text{S}$ are to be multiplied by 1.07 to agree with the more accurate values published by Bermejo et al. [107].

The self-broadened half-widths are based on the work of Bouanich et al. [102] and the air-broadened half-widths are based on Refs. [108–110]. Pressure shifts are all set to zero, but there is some new work in progress [111].

For the future, the HITRAN data for OCS will be improved in three main directions, on the basis of Refs. [90,91,96–98], and eventually of new measurements. First, the rotational spectra are to be extended to new isotopologues and to many excited vibrational states. Second, the intensities of the strongest infrared bands require further validations. Third, the infrared spectrum is to be extended beyond 4200 cm^{-1} , up to 8000 cm^{-1} .

2.20. H_2CO (molecule 20)

No changes in formaldehyde line parameters have been made since the previous edition of HITRAN [1].

2.21. HOCl (molecule 21)

No changes in hydrochlorous acid line parameters have been made since the previous edition of HITRAN [1]. A new line list in two spectral regions was created, but transcription for HITRAN was not completed in time for the HITRAN2k update. The list corresponds to the pure-rotation lines [112] and the ν_2 region from 1178 to 1321 cm^{-1} [113].

2.22. N₂ (molecule 22)

No changes in nitrogen line parameters have been made since the previous edition of HITRAN [1].

2.23. HCN (molecule 23)

No changes in hydrogen cyanide line parameters have been made since the previous edition of HITRAN [1]. However, a major update has been in progress for HCN. Line positions and intensities throughout the infrared have been revisited by Maki et al. [114,115]. These data will greatly increase the number of bands in HITRAN. The collision-broadening parameters and shifts are being updated based upon the studies by Devi et al. [116] and by Rinsland et al. [117].

2.24. CH₃Cl (molecule 24)

No changes in methyl chloride line parameters have been made since the previous edition of HITRAN [1]. A line list for the ν_2 , ν_5 and $2\nu_3$ vibrational band triad covering the 6- to 8- μm region has been prepared, based upon the work of Chackerian et al. [118].

2.25. H₂O₂ (molecule 25)

No changes in hydrogen peroxide line parameters have been made since the previous edition of HITRAN [1]. A preliminary line list covering 0–1427 cm^{-1} has been prepared by Perrin et al. [119,120]. These data are being converted into the HITRAN format.

2.26. C₂H₂ (molecule 26)

Three spectral regions have had major updates for the current edition. These updates cover the 13.6- μm region (600–870 cm^{-1}), the 7.5- μm region (1248–1415 cm^{-1}), and the 5- μm region. The extensive improvements and additions to HITRAN, as well as future recommendations, are described in [5].

A larger and more standardized notation has been adopted for acetylene in order to describe the many additional vibrational energy levels for the upper states in the 5- μm region. Table 7 lists the levels that are now in HITRAN, illustrating the 8-character ASCII representation adopted in HITRAN (also see the notes of Table 3). Two levels (000(11)₊⁰ and 000(11)₋⁰) were unfortunately given the same vibrational index in HITRAN; the identifications are being corrected for the next

Table 7

Vibrational notation for acetylene adopted in HITRAN

Vibrational level	HITRAN notation $v_1v_2v_3v_4v_5l \pm r$	Vibrational level	HITRAN notation $v_1v_2v_3v_4v_5l \pm r$
Ground state	000000+	000(31) ₋ ⁰	000310–
000(01) ¹	000011	000(31) ² II	000312 2
001(00) ₊ ⁰	001000+	000(31) ² I	000312 1
010(11) ₊ ⁰	010110+	010(01) ¹	010011
000(10) ¹	000101	000(13) ₊ ⁰	000130+
000(11) ₊ ⁰	000110+	000(13) ₋ ⁰	000130–
000(11) ₋ ⁰	000110–	000(13) ² II	000132 2
000(11) ²	000112	000(13) ² I	000132 1
000(02) ₊ ⁰	000020+	010(10) ¹	010101
000(02) ²	000022	000(22) ₊ ⁰ II	000220+2
000(03) ¹	000031	000(22) ₋ ⁰	000220–
000(21) ¹ II	000211 2	000(22) ² II	000222 2
000(21) ¹ I	000211 1	000(04) ₊ ⁰	000040+
000(31) ₊ ⁰	000310+	000(04) ²	000042

edition. Only the first 10 levels for C₂H₂ in the table were present in earlier editions of HITRAN [1,2]. More complete statistics of the acetylene bands present in HITRAN are given in Ref. [5].

2.27. C₂H₆ (molecule 27)

No changes in ethane line parameters have been made since the previous edition of HITRAN [1]. The parameters in HITRAN for ethane are quite dated. A modified line list [121] for the ^PQ₃ sub-branch in the ν_7 band of ethane will be incorporated in a future edition of HITRAN. It contains line positions, intensities, lower-state energies, air-broadening and air-pressure shift coefficients. The results of the new analysis represent significant improvements over those used for earlier atmospheric studies.

2.28. PH₃ (molecule 28)

No changes in phosphine line parameters have been made since the previous edition of HITRAN [1]. A review of the status of spectral line parameters of this molecule is presented [73] in this Special Issue and a new line list is forthcoming.

2.29. COF₂ (molecule 29)

No changes in carbonyl fluoride line parameters have been made since the previous edition of HITRAN [1]. A new line list for the 5.1- μ m region has been generated by Brown [122]. Much of the analysis has gone into determining the intensities.

2.30. SF_6 (molecule 30)

No changes in sulfur hexafluoride line parameters have been made since the previous edition of HITRAN [1]. The old parameters for this species have been placed in a supplemental folder in the compilation, as discussed at the beginning of this section.

2.31. H_2S (molecule 31)

The spectral line parameters for the ν_1 and ν_3 fundamentals of hydrogen sulfide have been replaced [123]. The new line list also includes numerous combination and hot bands, introduced into HITRAN for the first time. Unfortunately, in the official HITRAN2k file for H_2S , the reference to these bands for positions and intensities [123] did not get recorded on the lines.

Significant improvements to the air- and self-broadened half-widths should still be made. It has been recommended [124] that the value of $\gamma_{\text{air}} = 0.08 \text{ cm}^{-1} \text{ atm}^{-1}$ would be preferable to the current default value of $0.15 \text{ cm}^{-1} \text{ atm}^{-1}$ for transitions above 2000 cm^{-1} . Even better results would be obtained by adopting the work of Kissel et al. [125].

2.32. $HCOOH$ (molecule 32)

No changes in formic acid line parameters have been made since the previous edition of HITRAN [1]. Line parameters in the ν_6 region from the work of Perrin et al. [126] are being considered for the next HITRAN edition.

2.33. HO_2 (molecule 33)

The line parameters for the rotational lines of the hydroperoxyl radical have been updated in the present edition of HITRAN. The new line positions are based upon the work of Chance et al. [127]. Intensities use direction cosine matrix elements from this work, and the dipole-moment measurements of Saito and Matsumura [128]. The update extends the spectral coverage from the previous value of 334 cm^{-1} to 909 cm^{-1} . These new data include all rotational transitions up to $N = 30$ and $K_a = 9$.

The air-broadened half-width of all lines of HO_2 have been changed from the generic $0.05 \text{ cm}^{-1} \text{ atm}^{-1}$ used previously to the value of $0.107 \text{ cm}^{-1} \text{ atm}^{-1}$ [129].

2.34. O (molecule 34)

No changes for the oxygen atom lines have been made since the previous edition of HITRAN [1].

2.35. $ClONO_2$ (molecule 35)

No changes in chlorine nitrate line parameters have been made since the previous edition of HITRAN [1]. The previous line parameters for this molecule have been placed in a supplemental folder in the compilation, as discussed at the beginning of this section.

2.36. NO^+ (molecule 36)

No changes for the ionic species NO^+ line parameters have been made since the previous edition of HITRAN [1].

2.37. HOBr (molecule 37)

No changes in hydrobromous acid line parameters have been made since the previous edition of HITRAN [1].

2.38. C_2H_4 (molecule 38)

The spectral line parameters for ethylene are a new addition to HITRAN. This new linelist contains 8 bands for the main isotopologue, $^{12}\text{C}_2\text{H}_4$, and two bands for the isotopologue $^{12}\text{C}^{13}\text{CH}_4$. For the main isotopologue the bands included are: ν_{10} , ν_7 , ν_4 , ν_9 , ν_{11} , $\nu_2 + \nu_{12}$, $2\nu_{10} + \nu_{12}$, $\nu_9 + \nu_{10} - \nu_{10}$. For the second isotopologue, the bands included are the ν_9 band and the ν_{11} bands. The data cover the spectral region from 700 to 3243 cm^{-1} . The line positions are taken from Refs. [130–133], while the intensities are from Refs. [130,133–135]. Values for pressure-broadening coefficients have been taken from the work of Brannon and Varanasi [136]. A value of $0.09\text{ cm}^{-1}\text{ atm}^{-1}$ has been chosen for the self-broadened width throughout the linelist. A value of 0.82 has been adopted throughout for the temperature-dependence exponent of the air-broadened half-width, n [136]. No pressure-shift coefficients have been reported.

3. IR cross-sections

The number of molecules and the extent of the data represented by IR cross-sections in HITRAN have increased rapidly. The cross-sections are generally used for polyatomic molecules that possess low-lying fundamentals, often on the order of kT or lower. Cross-sections are also used for “heavy” molecular species, whose spectral lines are unresolved in the laboratory, and are likewise extremely difficult to calculate. Cross-sections also have the advantage of incorporating various spectroscopic effects, such as line coupling, pressure shifts, etc. On the downside however, the cross-sections may include undesired contributions from the apparatus function of the spectrometer used in the laboratory. A discussion of the units is given in the previous HITRAN article [1]. A slightly more standardized header for each temperature–pressure set has been implemented; the format is shown in Table 8.

The cross-sections are derived from laboratory measurements using Fourier transform spectrometers. The cross-sections have been cast into an equal wavenumber interval grid. It should be noted that the initial and final wavenumbers, ν_{\min} and ν_{\max} , respectively, of each temperature–pressure set for a given wavenumber region are not always identical. They have been taken from the analysis of the observations. The sampling intervals are also not necessarily identical. The wavenumber interval of the grid is obtained by taking the difference of the initial and final wavenumber and dividing this quantity by the number of points, N , minus one, i.e., $\Delta\nu = (\nu_{\max} - \nu_{\min}) / (N - 1)$.

Table 8
Format for cross-section headers for each temperature–pressure set

Quantity	Field length	Type	Comment
Molecule	20	Hollerith	Chemical formula (right-justified)
Minimum wavenumber	10	Real	Start of range (cm^{-1})
Maximum wavenumber	10	Real	End of range (cm^{-1})
Number of points	7	Integer	Number of cross-sections in set
Temperature	7	Real	Temperature (K) of set
Pressure	6	Real	Pressure of set in Torr
Maximum cross-section value in the set	10	Real	Useful for scaling plots ($\text{cm}^2/\text{molecule}$)
Instrument resolution	5	Real	See note
Common name	15	Hollerith	Familiar name of molecule
Not currently used	4		Reserved for future use
Broadener	3	Hollerith	“Air”, or self-broadened if left blank
Reference	3	Integer	Index pointing to source of data

Note: Most cross-sections were taken from FTS measurements. In that case the resolution is given in cm^{-1} . There are some cross-sections taken from grating spectrometer measurements in the UV. In those cases, the resolution is given in milliångströms in the form $xxx\text{ m}\text{\AA}$, where xxx are up to three digits.

Table 9 lists the molecules that presently have IR cross-sections in HITRAN2k. Ideally, for atmospheric simulation purposes a reasonably large set of temperatures and pressures at each spectral range would be desired. The third column of Table 9 gives the overall temperature range of the temperature–pressure sets, while column four gives the total pressure range. For many molecules, measurements are only available for the pure sample, indicated by a total pressure of zero in Table 9. As can be seen in the fifth column, the spectral coverage of the data in HITRAN is in the spectral region of 5.6–17.2 μm .

Although hydrohalocarbons are present in very small amounts in the present-day atmosphere, some have reached the minimum concentration levels required to be measured in the ambient air. As the emissions of hydrohalocarbons are expected to increase in the future due to international regulation of CFC emission (Montreal protocol and further amendments), high-resolution temperature-dependent cross-sections are needed for determining the atmospheric concentrations using infrared spectroscopy. As reported in [151], it is important to know the temperature dependence of the spectral features in order to derive accurate concentrations.

Atmospheric abundances of CFCs have already been determined by Fourier transform infrared (FTIR) spectroscopy using laboratory spectroscopic data both from ground-based measurements [152] or balloon-borne experiments [153]. Recent simulations by Coheur et al. [154], using CFC and CFC-substitute emission scenarios from WMO/IPCC, show that a current space-borne nadir FTIR instrument could detect CFC-12 (and possibly CFC-11 and HCFC-22 when averaging on wide geographical areas), whereas limb or solar-occultation FTS instruments already detect CFC-11, CFC-12, HCFC-22, CFC-113 and should measure HFC-134a and HCFC-142b after 2005 when their atmospheric concentrations have increased.

The uncertainties associated with the cross-sections provided in [147], which were determined from measurements made at 0.03 cm^{-1} resolution, range from 1–2% for strong absorptions to 3–4%

Table 9
Summary of molecules represented by IR cross-section data in HITRAN

Molecule	Common name	Temperature range (K)	Pressure range (Torr)	Number of T, P sets	Spectral coverage (cm^{-1})	Sources (Refs.)
SF ₆	Sulfur hexafluoride	180–295	20–760	32	925–955	137,138
		189–297	0–155	23	740–840	139
ClONO ₂	Chlorine nitrate	189–297	0–156	23	1250–1330	139
		213–296	0	2	1680–1790	140
CCl ₄	Carbon tetrachloride	208–297	8–760	32	750–812	141
N ₂ O ₅	Dinitrogen pentoxide	205–293	0	5	699–799	139
		205–293	0	5	1199–1279	139
HNO ₄	Pernitric acid	268	0.7	1	770–830	142
C ₂ F ₆	Hexafluoroethane, CFC-116	181–296	25–760	43	1061–1165	143
		181–296	25–760	43	1220–1285	143
CCl ₃ F	CFC-11	190–296	8–760	55	810–880	138, 144
		190–296	8–760	55	1050–1120	138, 144
CCl ₂ F ₂	CFC-12	190–296	8–760	52	850–950	138
		190–296	8–760	52	1050–1200	138
CClF ₃	CFC-13	203–293	0	6	765–805	145
		203–293	0	6	1065–1140	145
		203–293	0	6	1170–1235	145
CF ₄	CFC-14	180–296	8–761	55	1250–1290	146
C ₂ Cl ₃ F ₃	CFC-113	203–293	0	6	780–995	145
		203–293	0	6	1005–1232	145
C ₂ Cl ₂ F ₄	CFC-114	203–293	0	6	815–860	145
		203–293	0	6	870–960	145
		203–293	0	6	1030–1067	145
		203–293	0	6	1095–1285	145
C ₂ ClF ₅	CFC-115	203–293	0	6	955–1015	145
		203–293	0	6	1110–1145	145
		203–293	0	6	1167–1260	145
CHCl ₂ F	HCFC-21	296	1	1	785–840	142
CHClF ₂	HCFC-22	181–297	0–765	29	760–860	138, 147
		181–296	22–761	31	1070–1195	138
		253–287	0	3	1060–1210	147
		253–287	0	3	1275–1380	147
CHCl ₂ CF ₃	HCFC-123	253–287	0	3	740–900	147
		253–287	0	3	1080–1450	147
CHClFCF ₃	HCFC-124	287	0	1	675–715	147
		287	0	1	790–920	147
		287	0	1	1035–1430	147
CH ₃ CCl ₂ F	HCFC-141b	253–287	0	3	710–790	147
		253–287	0	3	895–1210	147
		253–287	0	3	1325–1470	147
CH ₃ CClF ₂	HCFC-142b	253–287	0	3	650–705	147
		253–287	0	3	875–1265	147
		253–287	0	3	1360–1475	147
CHCl ₂ CF ₂ CF ₃	HCFC-225ca	253–287	0	3	695–865	147
		253–287	0	3	1010–1420	147

Table 9 (continued)

Molecule	Common name	Temperature range (K)	Pressure range (Torr)	Number of T, P sets	Spectral coverage (cm^{-1})	Sources (Refs.)
$\text{CClF}_2\text{CF}_2\text{CHClF}$	HCFC-225cb	253–287	0	3	715–1375	147
CH_2F_2	HFC-32	203–297	0–750	17	995–1236	148
		203–297	0–750	17	1385–1475	148
CHF_2CF_3	HFC-125	287	0	1	700–745	147
		287	0	1	840–890	147
		287	0	1	1060–1465	147
CHF_2CHF_2	HFC-134	203–297	0–750	9	600–1700	149
CFH_2CF_3	HFC-134a	253–287	0	3	815–865	147
		190–296	20–760	32	1035–1130	150
		190–296	20–760	33	1135–1340	150
		253–287	0	3	935–1485	147
CF_3CH_3	HFC-143a	203–297	0–750	9	580–630	149
		203–297	0–750	9	750–1050	149
		203–297	0–750	9	1100–1500	149
CH_3CHF_2	HFC-152a	253–287	0	3	840–995	147
		253–287	0	3	1050–1205	147
		253–287	0	3	1320–1490	147

Note: These data are in the main directory. Additional redundant data [145] for CFC-11 and CFC-12 are stored in a supplemental sub-directory (see Fig. 1).

for weak absorptions. They were obtained by adding the uncertainties due to the following sources of error: pressure and temperature measurements, purity determination, and path length.

Depending upon the sample used, the volumetric purity of the gas sample varied between 99% and 99.99%. The uncertainty in the cell length that was measured by interferometric method was about 0.2%. The uncertainties in the pressure measurements were better than 0.15% and the temperature measurement was accurate to ± 0.2 K. Total uncertainties associated with integrated absorption intensities of bands are also provided in Ref. [147].

Very comprehensive pressure–temperature sets of numerous species have been adopted for the HITRAN compilation from the laboratory studies carried out at the State University of New York at Stony Brook [137–144, 146, 148–150]. The wavenumber scales of the high-resolution Fourier transform spectra were calibrated using the absorption lines of ammonia, acetylene, carbon dioxide, methane, and nitrous oxide bands in the thermal infrared (7–14 μm) as given in HITRAN. The total (atmospheric) pressures were accurate to 0.1% of the value quoted in hPa. For example, 30 hPa could be 30 ± 0.03 hPa.

The uncertainty in the volumetric mixing ratios, which directly affect the measured value of the cross-sections of the absorbing molecules, was 0.14%. The transmittance was measured with an uncertainty less than 0.3%. The S/N ratio in the measurement of the transmittance was always 300:1 or better. The uncertainty of the optical path length was about 1%. This also affects the measured cross-section. The temperature of the gas (190–296 K) was known to an accuracy better than 0.5 K. Spectral resolution was chosen judiciously so that instrumental distortion of the measured spectra did not enter into the scheme of things that was devised for measuring the cross-sections. With

all these sources of error specified, a simple statistical analysis [146] yields the estimated absolute experimental (or systematic) error in the reported cross-sections.

Sources of uncertainty in IR cross-section measurements have also been investigated in a detailed study involving a number of other groups led by the Rutherford Appleton Laboratory. The results for HCFC-22 and recommendations for improving such measurements are summarized by Ballard et al. [155].

4. Ultraviolet data sets

Ultraviolet data sets in the HITRAN compilation are divided into two categories, line-by-line and cross-sections, as shown in Fig. 1. In addition to the new data described below, it is now possible to access other data sets not included in HITRAN by using features of the software described in Section 6 of this paper.

4.1. Line-by-line parameters

Data in the UV are now provided for the first time in the HITRAN compilation for the hydroxyl radical. The line parameters for the $A^2\Sigma^+ \leftarrow X^2\Pi$ bands of OH cover the region 29 808–35 877 cm^{-1} . They are described in the work of Gillis et al. [156].

4.2. UV Cross-sections

An extensive list of cross-sections for nitrogen dioxide, NO_2 , appears in HITRAN for the first time. The cross-sections are taken from measurements of Vandaele et al. [157]. They cover the spectral region from 15 000 to 42 000 cm^{-1} (238–666 nm) at two temperatures, 220 and 294 K.

5. Aerosols

Optical depth in the atmosphere is comprised of contributions from both gas species and aerosol particles. Aerosol particles are present throughout the atmosphere, from the surface to the mesopause, and include liquid and solid particles of various sizes, shapes, and composition.

A size distribution of particles of a single composition has an extinction coefficient k_{ext} (km^{-1}) that contributes an increment of optical depth $k_{\text{ext}} ds$ over a path length ds (km). In the spherical approximation, the extinction coefficient is given by

$$k_{\text{ext}} = 1.0 \times 10^{-3} \int Q_{\text{ext}}(x, m(\lambda)) \pi r^2 dN/dr dr, \quad (1)$$

where Q_{ext} is the Mie efficiency factor for extinction (dimensionless), r the particle radius (μm), and dN/dr the particle size distribution (particles $\text{cm}^{-3} \mu\text{m}^{-1}$). The factor 1.0×10^{-3} is used to convert k_{ext} to the km^{-1} unit. Q_{ext} is a function of the complex index of refraction $m = m_{\text{real}} + im_{\text{imag}}$, and $x = 2\pi r/\lambda$ is the particle size parameter (dimensionless), where λ is the wavelength (μm). Both the real (m_{real}) and imaginary (m_{imag}) parts of the complex index of refraction are included in the HITRAN compilation for many substances.

Table 10
Indices of refraction in the HITRAN2k compilation

Substance	Comments
Water (liquid)	0.65–1000 μm
Water (ice)	0.04–8 $\times 10^6$ μm
Water (ice)	Water ice 800–4004 cm^{-1} from 130 to 210 K
Liquid $\text{H}_2\text{SO}_4/\text{H}_2\text{O}$	Room temperature and cold temperature data
Liquid $\text{HNO}_3/\text{H}_2\text{O}$	Room temperature and cold temperature data
α NAT	1.4–20 μm , nitric acid trihydrate solid film at 196 K
β NAT	Indices from two laboratories, at 160 and 196 K
NAD	1.4–20 μm , nitric acid dihydrate solid film at 184 K
NAM	1.4–20 μm , nitric acid trihydrate solid film at 179 K
aNAT	Amorphous NAT solid solution film at 153 K
aNAM	Amorphous NAM solid solution film at 153 K
NaCl	Room temperature, 0.2–30 000 μm
Sea salt	Room temperature, 0.2–30 000 μm
Ammonia sulfate	Room temperature, 0.2–30 000 μm
Carbonaceous material	Room temperature, 0.2–30 000 μm
Volcanic dust	Room temperature, 0.2–30 000 μm
Meteoritic dust	Room temperature, 0.2–30 000 μm
Quartz	Room temperature, 0.2–30 000 μm
Iron oxide	Room temperature, 0.2–30 000 μm
Sand	Room temperature, 0.2–30 000 μm
Aqueous $\text{HNO}_3/\text{H}_2\text{O}$	Three tabulations, temperatures from room to 213 K
Aqueous $\text{H}_2\text{SO}_4/\text{H}_2\text{O}$	Five tabulations, temperatures from room to 200 K
Organic non-volatile aerosol	Indices for burning vegetation

Scattering and absorption coefficients, analogous to Eq. (1), are expressed by integrals that contain the Q_{sca} and Q_{abs} Mie efficiency factors [158]. For an atmosphere that has particles that scatter as well as absorb, radiative transfer in the atmosphere is described by a source function that has both thermal emission and scattering terms [159]. Particles (both liquid and solid) complicate the calculation and interpretation of remote sensing radiation fields, since particle effects are dependent upon particle size (as specified by the particle size distribution), shape (e.g. cirrus particles are non-spherical), composition (the wavelength dependence of the refractive index is dependent upon composition), angular dependencies (as specified by the phase function of the particles), and the scattering properties at a specified location (i.e., the ratio of $k_{\text{sca}} ds$ to the sum of the local gas and particle optical depth).

The HITRAN database compiles indices of refraction for many particle composition types. A summary of the aerosol files in HITRAN2k is contained in the document located at <ftp://cfa-ftp.harvard.edu/pub/HITRAN/Aerosols/Aerosol-Readme.pdf>. Additional information is in the article by Massie and Goldman [160]. A brief listing of the files is given in Table 10. The aerosol files contain information that identifies the contents of the file (composition, wavenumber, and temperature ranges), specifies the original journal reference, identifies an email contact, and specifies the Fortran format of the data. The data are tabulated at the resolution of the original measurements (the data have not been interpolated to a common wavenumber grid).

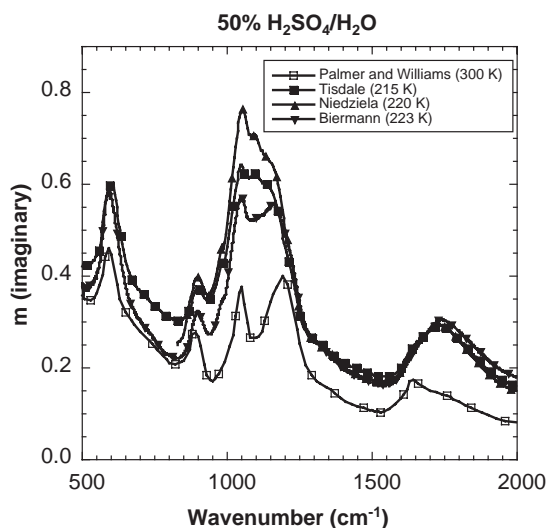


Fig. 4. The imaginary indices of refraction of 50% $\text{H}_2\text{SO}_4/\text{H}_2\text{O}$ (by weight) at room temperature [168], and cold stratospheric temperatures [164–166].

In some cases, data from several sources have been provided. For example, Toon et al. [161] and Richwine et al. [162] indices for nitric acid trihydrate (NAT), measured at 196 and 160 K, are both included in the compilation. The inclusion of both data sets allows the user to assess the differences between the various measurements. These differences, when translated into aerosol extinction calculations, are helpful to assess uncertainties in the modeling of aerosol extinction spectra. Also, since indices of refraction are temperature dependent, differences in measurements at various temperatures may reflect actual temperature-dependent effects.

Discussions of the indices, present in previous HITRAN compilations, and also included in HITRAN2k, are given in [1,163]. Previous compilations primarily tabulated indices at room temperatures. Interest in the indices at stratospheric temperatures has been motivated by the role of heterogeneous chemistry in the polar regions. Liquid and solid polar stratospheric cloud particles transform inactive chlorine into active chlorine in the polar regions of the stratosphere. Interpretation of infrared and visible remote sensing observations of these particles requires cold temperature indices of refraction for several particle types. Liquid droplets of $\text{H}_2\text{SO}_4/\text{H}_2\text{O}$ incorporate HNO_3 to become ternary ($\text{HNO}_3/\text{H}_2\text{O}/\text{H}_2\text{SO}_4$) droplets at temperatures colder than 195 K at 20 km. The formation of solid nitric acid trihydrate (NAT), dihydrate (NAD), and water ice particles also occurs as temperatures become increasingly colder.

Laboratory studies during the last several years have led to the publication of indices of refraction for $\text{H}_2\text{SO}_4/\text{H}_2\text{O}$ droplets [164–166] and $\text{HNO}_3/\text{H}_2\text{O}$ [166,167] at stratospheric temperatures. The imaginary part of the $\text{H}_2\text{SO}_4/\text{H}_2\text{O}$ index for 50% H_2SO_4 by weight at room temperature and temperatures near 220 K is presented in Fig. 4 for four data sets, to illustrate the current status of the cold-temperature indices. The imaginary index is presented since the wavelength dependence of the extinction spectrum in the infrared for $\text{H}_2\text{SO}_4/\text{H}_2\text{O}$ (and other particles for which the particle size parameter x is less than unity) is closely related to the wavelength dependence of the imaginary

index. The room temperature values of Palmer and Williams [168] are considerably less than those of the cold temperature values. Though the cold temperature values are closer to each other in value than the room temperature data, there are important differences between the cold temperature data that need to be reconciled by additional studies.

Since the current tabulation is at discrete temperatures, the development of a semi-empirical specification of the real and imaginary indices for $\text{H}_2\text{SO}_4/\text{H}_2\text{O}$, $\text{H}_2\text{SO}_4/\text{HNO}_3$, and $\text{H}_2\text{SO}_4/\text{HNO}_3/\text{H}_2\text{O}$ over a range of temperature and conditions (e.g. weight percent H_2SO_4 and HNO_3), is a desired future goal. The accuracy of such a parameterization will of course be dependent upon the discrete measurements, for which current differences were noted in the preceding paragraph.

6. Software and associated features of the HITRAN compilation

The current release of the database contains a subdirectory called Software, as shown in Fig. 1. The installers of the software for different platforms are located in this directory. Under this subdirectory, there are two other subdirectories, which are Documentation and Generic. Below are descriptions of the software and files in the Documentation and Generic directories.

6.1. HITRAN software JavaHAWKS

The suite of stand alone software included in HAWKS provides database management functions such as filtering, plotting, and manipulation of the HITRAN and associated molecular databases. It does not provide atmospheric modeling, although a widely used function in the software is to create files for subsequent input to radiance codes. Before the release of HITRAN96 [1], the software utilized to work with HITRAN was written in the C programming language and was named cHAWKS. Because C is platform dependent, different versions of cHAWKS had to be maintained so that the software could work on different platforms such as Windows, Unix/Linux systems, and Macintosh operating systems.

The current HITRAN software is called JavaHAWKS, which is a Java version of HAWKS. This migration from cHAWKS to JavaHAWKS occurred after HITRAN96 [1] and marked a significant improvement in maintaining HITRAN software. Since Java is a platform-independent programming language, JavaHAWKS is a complete cross-platform application. This makes it possible to maintain a single source code for the HITRAN software and thus to provide the same performance for the different platforms.

JavaHAWKS provides functionality that allows the user to perform the following major operations: (1) select data from the line-by-line or cross-section portions of the database; (2) display and print stick plots of line intensities or energy levels; (3) directly access the HITRAN files located on the HITRAN web server; (4) select and convert spectral lines from other databases, e.g. the JPL catalog [169] and the extensive UV data files located at the Atomic and Molecular Physics Division of the Harvard-Smithsonian Center for Astrophysics, into HITRAN-format files; (5) directly link to the HITRAN website update page and ftp-site; (6) find journal references for line positions, intensities, and half-widths; and (7) have extensive access to the historical documentations of the HITRAN database. Operations 1, 2, and 6 are stand alone applications which are performed on the user's

local machine. Operations 3, 4 and 5 require the user to have an internet connection and an installed web browser. Fig. 5 shows some of the pull-down menu features that can be used in JavaHAWKS.

There are six files under the Software subdirectory. They are: (1) Win_Setup.exe; (2) Linux_Setup.bin; (3) Unix_Setup.bin; (4) MacOS_Setup.bin; (5) MacOSX_Setup.zip; and (6) Software-Readme. The first five files are JavaHAWKS installers for different operating systems. These installation files of JavaHAWKS are distributed via the HITRAN ftp-site (<ftp://cfa-ftp.harvard.edu/pub/HITRAN/Software/>) without charge. The file Win_Setup.exe is for the PC, Linux_Setup.bin is for Linux, Unix_Setup.bin is for any generic Unix system (e.g. Solaris, Linux, Unix, etc), MacOS_Setup.bin is for any Macintosh with operating system from 8.x to 9.x, and MacOSX_Setup.zip is for Macintosh with OS X operating system. Based on the platform the user is using, a proper installer should be downloaded from the HITRAN ftp-site. Compared to previous installers of JavaHAWKS, these will greatly simplify the procedures of installing JavaHAWKS on the user's computer, especially for Macintosh users. After the completion of downloading a proper installer, depending on the platform, the user should click on the downloaded file or run the downloaded file from the command line. This will lead to the procedures of the JavaHAWKS installation. A description of the installation procedures for different platforms can be found in the Software-Readme file under the Software subdirectory. A complete description of the software and operating instructions is given in the JavaHAWKS manual which is located in the folder Documentation of the Software subdirectory and is described below. The JavaHAWKS installation files are occasionally updated. The most recent version can be obtained from the HITRAN ftp-site.

6.2. Documentation

A comprehensive user's manual is provided with the JavaHAWKS software. It is designed to assist the user in easily adapting to the manipulation of the HITRAN molecular spectroscopic database and associated molecular databases by proper utilization of the JavaHAWKS software package. It includes installation instructions for the Windows, Unix/Linux, and Macintosh, and a detailed description of the capabilities of the JavaHAWKS software.

The JavaHAWKS manual, in pdf format, is provided in the Documentation folder. The user can also access the manual within the JavaHAWKS software. The manual is located under the main menu item HELP of the JavaHAWKS software (see Fig. 5).

The file ref-table2003.pdf, also stored under the Documentation subdirectory, lists the references from journals, personal communications, or unpublished data for the line positions, intensities, and half-widths of related spectral lines, as well as references for the cross-sections and band centers. A comprehensive collection of the abstracts for those published references is reflected in the pdf file called ReferenceTable.pdf. This file can be accessed from within the JavaHAWKS software simply by clicking on ReferenceTable.pdf from the main menu item HELP (see Fig. 5). Within the pdf file, clicking on the first author in the reference table will link you to the corresponding abstract of the article.

From the HELP menu of the JavaHAWKS software, the user can also access historical HITRAN documentations dating back to the original 1973 report as well as recent HITRAN conference proceedings.

Considerable care has been exercised in identifying the original sources of data included in the database, and in identifying the nature of the data (e.g., whether they are experimental or theoretical

in nature). The users of the database are urged to identify the original sources of the data along with the database itself, by following the reference pointers provided. Referencing the efforts of authors who contributed their data to HITRAN is essential for the continuing progress in spectroscopy necessary to address the deficiencies that exist for many applications.

6.3. Auxiliary data files

There are data in the HITRAN compilation that are general in nature and hence have been placed in tables external to the line-by-line portion of the database. One of these is called *molparam.txt*. This file contains the abundance factors adopted from Ref. [3] for all the isotopologues in HITRAN. The table also presents for these species the partition sum at 296 K, the state-independent statistical weight, and the molar mass. Another external table to HITRAN is called *bandcent.dat*. This file is a list of the bands in HITRAN (often with the band centers in wavenumbers). It is used as an input for one of the features in JavaHAWKS that allows the user to query a HITRAN-like file for various statistics and extrema of parameters. There is also a directory in the ftp-site that contains files for each isotopologue in HITRAN (as well as a few additional rare isotopologues) with the partition sums at one-degree intervals from 70 to 3000 K. The description of the calculational scheme for the partition sums is given in Ref. [170].

6.4. Future enhancements to software

The requirements of spectroscopic applications, as well as the improvements in both laboratory and theoretical efforts, are mandating a change in the format of HITRAN. The next edition will advance from the 100-character per transition record employed since 1986 to a 160-character record. The Einstein-A coefficient will replace the square of the transition probability and the upper- and lower-statistical weights of the levels of a transition will be given. The format will make the quantum identifications more transparent. Accuracies and references for the self-broadened half-width, the temperature dependence of the air-broadened half-width, and the pressure shift will be given.

The software for the next edition will have many more useful features, not only for dealing with the expanded HITRAN line-by-line and cross-section database, but also for accessing other relevant spectral catalogs and casting them into the HITRAN standardized format. We are implementing an internet version of JavaHAWKS that works from a server at the Harvard-Smithsonian Center for Astrophysics. The installation process for the stand-alone version of JavaHAWKS is also being simplified.

Acknowledgements

The HITRAN molecular database has been a project with strong international cooperation during its development. Laboratories throughout the world have contributed both experimental data and theoretical calculations. We in particular want to acknowledge the major contributions of C. Chackerian, E.A. Cohen, P.F. Coheur, H. Dothe, J. Fischer, L.P. Giver, D. Goorvitch, I. Kleiner, K. Minschwaner, D. Nelson, and J. Orphal. A. Berk, J.W. Brault, A. Chursin, J.W. Hannigan, T. Heinemann,

H.-D. Holweg, and S. Mikhailenkov were instrumental in discovering correctable errors in HITRAN2k. We wish to especially thank M.D. King, D.O'C. Starr, and T.S. Cress for their support of this project.

The current effort has been supported by the NASA Earth Observing System (EOS), grant NAG5-8420; the NASA Upper Atmospheric Research Satellite (UARS) program; the Biological and Environmental Research Program (BER), US Department of Energy, Grant No. DE-FG02-00ER62930; and internal funding from the Smithsonian Institution.

References

- [1] Rothman LS, Rinsland CP, Goldman A, Massie ST, Edwards DP, Flaud JM, Perrin A, Camy-Peyret C, Dana V, Mandin JY, Schroeder J, McCann A, Gamache RR, Wattson RB, Yoshino K, Chance K, Jucks K, Brown LR, Nemtchinov V, Varanasi P. The HITRAN molecular spectroscopic database and HAWKS (HITRAN Atmospheric Workstation): 1996 Edition. *JQSRT* 1998;60:665–710.
- [2] Rothman LS, Gamache RR, Goldman A, Brown LR, Toth RA, Pickett HM, Poynter RL, Flaud JM, Camy-Peyret C, Barbe A, Husson N, Rinsland CP, Smith MAH. The HITRAN database: 1986 edition. *Appl Opt* 1987;26:4058–97.
- [3] De Bievre P, Gallet M, Holden NE, Barnes IL. Isotopic abundances and atomic weights of the elements. *J Phys Chem Ref Data* 1984;13:809–91.
- [4] Rothman LS, Young LDG. Infrared energy levels and intensities of carbon dioxide—II. *JQSRT* 1981;25:505–24.
- [5] Jacquemart D, Mandin JY, Dana V, Claveau C, Vander Auwera J, Herman M, Rothman LS, Régalia-Jarlot L, Barbe A. The IR acetylene spectrum in HITRAN: update and new results. *JQSRT*, doi:10.1016/S0022-4073(03)00163-8.
- [6] Brown LR, Benner DC, Champion JP, Devi VM, Fejard L, Gamache RR, Gabard T, Hilico JC, Lavorel B, Loëte M, Mellau GC, Nikitin A, Pine AS, Predoi-Cross A, Rinsland CP, Robert O, Sams RL, Smith MAH, Tashkun SA, Tyuterev VG. Methane line parameters in HITRAN. *JQSRT*, doi:10.1016/S0022-4073(03)00155-9.
- [7] Toth RA. Water vapor measurements between 590 and 2582 cm^{-1} : line positions and strengths. *J Mol Spectrosc* 1998;190:379–96.
- [8] Toth RA. Analysis of line positions and strengths of H_2^{16}O ground and hot bands connecting to interacting upper states: (020), (100), and (001). *J Mol Spectrosc* 1999;194:28–42.
- [9] Toth RA. HDO and D_2O low pressure, long path spectra in the 600–3100 cm^{-1} region I. HDO line positions and strengths. *J Mol Spectrosc* 1999;195:73–97.
- [10] Toth RA. Air- and N_2 -Broadening parameters of water vapor: 604 to 2271 cm^{-1} . *J Mol Spectrosc* 2000;201:218–43.
- [11] Toth RA. Air- and N_2 -broadening parameters of HDO and D_2O , 709 to 1936 cm^{-1} . *J Mol Spectrosc* 1999;198:358–70.
- [12] Toth RA, Brown LR, Plymate C. Self-broadened widths and frequency shifts of water vapor lines between 590 and 2400 cm^{-1} . *JQSRT* 1998;59:529–62.
- [13] Remedios JJ, D.Phil thesis, Oxford University, Oxford, UK, 1990.
- [14] Tobin DC, Turner DD, Revercomb HE, Knuteson RO, Clough SA, Cady-Pereira K. Analysis of the AERI/LBLRTM QME. Twelfth ARM Science Team Meeting Proceeding, St Petersburg, FL, 8–12 April, 2002.
- [15] Tjemkes SA, Patterson T, Rizzi R, Shephard MW, Clough SA, Matricardi M, Haigh J, Hopfner M, Payan S, Trotsenko A, Scott N, Rayer P, Taylor J, Clerbaux C, Strow LL, DeSouza-Machado S, Tobin D, Knuteson R. The ISSWG line-by-line inter-comparison experiment. *JQSRT* 2003;77:433–53.
- [16] Giver LP, Chackerian C, Varanasi P. Visible and near-infrared H_2^{16}O line intensity corrections for HITRAN 96. *JQSRT* 2000;66:101–5.
- [17] Brown LR, Toth RA, Dulick M. Empirical line parameters of H_2^{16}O near 0.94 μm : positions, intensities and air-broadening coefficients. *J Mol Spectrosc* 2002;212:57–82.
- [18] Chevillard JP, Mandin JY, Flaud JM, Camy-Peyret C. H_2^{16}O : line positions and intensities between 9500 and 11500 cm^{-1} . The (041), (220), (121), (201), (102), and (003) interacting states. *Can J Phys* 1989;67:1065–84.

- [19] Partridge H, Schwenke DW. The determination of an accurate isotope dependent potential energy surface for water from extensive ab initio calculations and experimental data. *J Chem Phys* 1997;106:4618–39.
- [20] Chevillard JP, Mandin JY, Flaud JM, Camy-Peyret C. H_2^{18}O : line positions and intensities between 9500 and 11 500 cm^{-1} . The (0 4 1), (2 2 0), (1 2 1), (2 0 1), (1 0 2), and (0 0 3) interacting states. *Can J Phys* 1987;65:777–89.
- [21] Camy-Peyret C, Flaud JM, Mandin JY, Bykov A, Naumenko O, Sinitsa L, Voronin B. Fourier-transform absorption spectrum of the H_2^{17}O molecule in the 9711–11 335 cm^{-1} spectral region: the first decade of resonating states. *JQSRT* 1999;61:795–812.
- [22] Mérienne MF, Jenouvrier A, Hermans C, Vandaele AC, Carleer M, Coheur PF, Colin R, Fally S, Bach M. Water vapor line parameters in the 13 000–9250 cm^{-1} region. *JQSRT*, doi:10.1016/S0022-4073(03)00148-1.
- [23] Fally S, Coheur PF, Carleer M, Clerbaux C, Colin R, Jenouvrier A, Mérienne MF, Hermans C, Vandaele AC. Water vapor line broadening and shifting by air in the 26 000–13 000 cm^{-1} region. *JQSRT*, doi:10.1016/S0022-4073(03)00149-3; Coheur PF, Fally S, Carleer M, Clerbaux C, Colin R, Jenouvrier A, Mérienne MF, Hermans C, Vandaele AC. New water vapor line parameters in the 26 000–13 000 cm^{-1} region. *JQSRT* 2002;74:493–510.
- [24] Coheur PF, Clerbaux C, Carleer M, Fally S, Hurtmans D, Colin R, Hermans C, Vandaele AC, Barret B, De Maziere M, De Backer H. Retrieval of atmospheric water vapor columns from FT visible solar absorption spectra: evaluation of spectroscopic databases. *JQSRT*, doi:10.1016/S0022-4073(03)00150-X.
- [25] Tolchenov RN, Tanaka M, Tennyson J, Zobov NF, Shirin SV, Polyanski OL, Maurellis AN. Water line parameters in the near-infrared and optical. *JQSRT*, doi:10.1016/S0022-4073(03)00151-1.
- [26] Schermaul R, Brault JW, Canas AAD, Learner RCM, Polyanski OL, Zobov NF, Belmiloud D, Tennyson J. Weak line water vapour spectrum in the 13 200–15 000 cm^{-1} region. *J Mol Spectrosc* 2002;211:169–78; Schermaul R, Learner RCM, Newnham DA, Williams RG, Ballard J, Zobov NF, Belmiloud D, Tennyson J. The water vapour spectrum in the region 8600–15 000 cm^{-1} : experimental and theoretical studies for a new spectral line database. I: laboratory measurements. *J Mol Spectrosc* 2001;208:32–42; Schermaul R, Learner RCM, Newnham DA, Ballard J, Zobov NF, Belmiloud D, Tennyson J. The water vapour spectrum in the region 8600–15 000 cm^{-1} : experimental and theoretical studies for a new spectral line database. II: construction and validation. *J Mol Spectrosc* 2001;208:43–50.
- [27] Brault JW. Private communication, 2003.
- [28] Toth RA. Extensive measurements of H_2^{16}O line frequencies and strengths: 5750–7965 cm^{-1} . *Appl. Opt.* 1994;33:4851–67.
- [29] Lepère M, Henri A, Valentin A, Camy-Peyret C. Diode-laser spectroscopy: line profiles of H_2O in the region of 1.39 μm . *J Mol Spectrosc* 2001;208:25–31.
- [30] Parvitte B, Zéninari V, Pouchet I, Durry G. Diode laser spectroscopy of H_2O in the 7165–7185 cm^{-1} range for atmospheric applications. *JQSRT* 2002;75:493–505.
- [31] Gamache RR, Fischer J. Half-widths of H_2^{16}O , H_2^{18}O , H_2^{17}O , HD^{16}O , and D_2^{16}O : I. Comparison between isotopomers. *JQSRT* 2003;78:289–304.
- [32] Wattson RB, Rothman LS. Direct numerical diagonalization: wave of the future. *JQSRT* 1992;48:763–80.
- [33] Devi VM, Benner DC, Rinsland CP, Smith MAH. Absolute rovibrational intensities of $^{12}\text{C}^{16}\text{O}_2$ absorption bands in the 3090–3850 cm^{-1} spectral region. *JQSRT* 1998;60:741–70.
- [34] Giver LP, Brown LR, Chackerian Jr C, Freedman RS. The rovibrational intensities of five absorption bands of $^{12}\text{C}^{16}\text{O}_2$ between 5218 and 5349 cm^{-1} . *JQSRT* 2003;78:417–36; Kshirsagar RJ, Giver LP, Chackerian Jr C. rovibrational intensities of the $(00^0_3) \leftarrow (10^0_0)$ Dyad absorption bands of $^{12}\text{C}^{16}\text{O}_2$. *J Mol Spectrosc* 2000;199:230–5; Kshirsagar RJ, Giver LP, Chackerian Jr C, Brown LR. The rovibrational intensities of the $2\nu_3$ band of $^{12}\text{C}^{16}\text{O}^{18}\text{O}$ at 4639 cm^{-1} . *JQSRT* 1999;61:695–701.
- [35] Goldman A, Stephen TM, Rothman LS, Giver LP, Mandin J-Y, Gamache RR, Rinsland CP, Murcray FJ. The 1- μm CO_2 Bands and the $\text{O}_2(0-1)X^3\Sigma_g^- - a^1\Delta_g$ and $(1-0)X^3\Sigma_g^- - b^1\Sigma_g^-$ Bands in the earth atmosphere. *JQSRT*, doi:10.1016/S0022-4073(03)00153-5.
- [36] Henningsen J, Simonsen H. The $(22^0_1-00^0_0)$ Band of CO_2 at 6348 cm^{-1} : linestrengths, broadening parameters, and pressure shifts. *J Mol Spectrosc* 2000;203:16–27.
- [37] Aguir MBE, Perrin MY, Taine J. Variational calculation of energies of highly excited rovibrational states of $^{12}\text{C}^{16}\text{O}_2$. *J Mol Spectrosc* 2002;215:234–43.

- [38] Tashkun SA, Perevalov VI, Teffo JL, Bykov AD, Lavrentieva NN. CDS-1000, the high-temperature carbon dioxide spectroscopic databank. *JQSRT*, doi:10.1016/S0022-4073(03)00152-3.
- [39] Rinsland CP, Flaud JM, Perrin A, Birk M, Wagner G, Goldman A, Barbe A, De Backer-Barilly MR, Mikhailenko SN, Tyuterev VG, Smith MAH, Devi VM, Benner DC, Schreier F, Chance K, Orphal J, Stephen TM. Spectroscopic parameters for ozone and its isotopes: recent measurements, outstanding issues, and prospects for improvements to HITRAN. *JQSRT*, doi:10.1016/S0022-4073(03)00154-7.
- [40] Johns JWC, Lu Z, Weber M, Sirota JM, Reuter DC. Absolute intensities in the ν_2 fundamental of N_2O at 17 μm . *J Mol Spectrosc* 1996;177:203–10.
- [41] Daumont L, Claveau C, De Backer-Barilly MR, Hamdouni A, Régalia-Jarlot L, Teffo JL, Tashkun S, Perevalov VI. Line intensities of $^{14}\text{N}_2^{16}\text{O}$: the 10 micrometers region revisited. *JQSRT* 2002;72:37–55.
- [42] Toth RA. Line positions and strengths of N_2O between 3515 and 7800 cm^{-1} . *J Mol Spectrosc* 1999;197:158–87.
- [43] Daumont L, Vander Auwera J, Teffo JL, Perevalov VI, Tashkun SA. Line intensity measurements in $^{12}\text{N}_2^{16}\text{O}$ and their treatment using the effective dipole moment approach. *J Mol Spectrosc* 2001;208:281–91.
- [44] Fukabori M, Aoki TA, Aoki TE, Ishida H, Watanabe T. Measurements of the line strengths and half-widths of the (2–0) and (3–0) band of CO. Proceedings of the Fifth HITRAN Conference, Hanscom AFB, MA, USA, 23–25 September 1998.
- [45] Picqué N, Guelachvili G, Dana V, Mandin JY. Absolute line intensities, vibrational transition moment, and self-broadening coefficients for the 3–0 band of $^{12}\text{C}^{16}\text{O}$. *J Mol Struct* 2000;517–8:427–34.
- [46] Chackerian Jr C, Freedman RS, Giver LP, Brown LR. Absolute rovibrational intensities and self-broadening and self-shift coefficients for the $X^1\Sigma^+V=3 \leftarrow V=0$ Band of $^{12}\text{C}^{16}\text{O}$. *J Mol Spectrosc* 2001;210:119–26.
- [47] Sung K, Varanasi P. Intensities, collision-broadened half-widths, and collision-induced line shifts in the second overtone band of $^{12}\text{C}^{16}\text{O}$. *JQSRT*, doi:10.1016/S0022-4073(03)00015-3.
- [48] Zou Q, Varanasi P. New laboratory data on the spectral line parameters in the 1–0 and 2–0 bands of $^{12}\text{C}^{16}\text{O}$ relevant to atmospheric remote sensing. *JQSRT* 2002;75:63–92.
- [49] Malathy Devi V, Benner DC, Smith MAH, Rinsland CP, Mantz AW. Determination of self- and H_2 -broadening and shift coefficients in the 2–0 band of $^{12}\text{C}^{16}\text{O}$ using a multispectrum fitting procedure. *JQSRT* 2002;75:455–71.
- [50] L. Régalia, private communication, 2003.
- [51] Predoi-Cross A, Bouanich JP, Benner DC, May AD, Drummond JR. Broadening, shifting, and line asymmetries in the $2 \leftarrow 0$ band of CO and CO- N_2 : experimental results and theoretical calculations. *J Chem Phys* 2000;113:1–11.
- [52] Henningsen J, Simonsen H, Møgelberg T, Trudsø E. The $0 \rightarrow 3$ overtone band of CO: precise linestrengths and broadening parameters. *J Mol Spectrosc* 1999;193:354–62.
- [53] Swann WC, Gilbert SL. Pressure-induced shift and broadening of 1560–1630-nm carbon monoxide wavelength-calibration lines. *J Opt Soc Am B* 2002;19:2461–7.
- [54] Jacquemart D, Mandin JY, Dana V, Picqué N, Guelachvili G. A multispectrum fitting procedure to deduce molecular line parameters: application to the 3–0 band of $^{12}\text{C}^{16}\text{O}$. *Eur Phys J D* 2001;14:55–69.
- [55] Malathy Devi V, Benner DC, Smith MAH, Rinsland CP. Self-broadening and self-shift coefficients in the fundamental band of $^{12}\text{C}^{16}\text{O}$. *JQSRT* 1998;60:815–24.
- [56] Voigt S, Dreher S, Orphal J, Burrows JP. N_2 broadening in the $^{13}\text{C}^{16}\text{O}$ 2–0 band around 4167 cm^{-1} . *J Mol Spectrosc* 1996;180:359–64.
- [57] Hannigan J. Private communication, 2001.
- [58] Berk A. Private communication, 2002.
- [59] Lafferty WJ, Solodov AM, Lugez CL, Fraser GT. Rotational line strengths and self-pressure-broadening coefficients for the 1.27- μm , $a^1\Delta_g - X^3\Sigma_g$, $v=0-0$ band of O_2 . *Appl Opt* 1998;37:2264–70.
- [60] Smith KM, Newnham DA. Near-infrared absorption cross sections and integrated absorption intensities of molecular oxygen (O_2 , $\text{O}_2\text{-O}_2$, and $\text{O}_2\text{-N}_2$). *J Geophys Res* 2000;105: 7383–96.
- [61] Brown LR, Plymate C. Experimental line parameters of the oxygen *A* band at 760 nm. *J Mol Spectrosc* 2000;199: 166–79.
- [62] Mandin JY, Dana V, Régalia L, Barbe A, Thomas X. *A*-splittings and line intensities in the first overtone of nitric oxide. *J Mol Spectrosc* 1997;185:347–55.
- [63] Mandin JY, Dana V, Régalia L, Barbe A, Von der Heyden P. Lambda-splittings and line intensities in the $3 \leftarrow 1$ hot band of $^{14}\text{N}^{16}\text{O}$: the spectrum of nitric oxide in the first overtone region. *J Mol Spectrosc* 1998;187:200–5.
- [64] Gillis JR, Goldman A. Nitric oxide IR line parameters for the upper atmosphere. *Appl Opt* 1982;21:1616–27.

- [65] Allout MY, Dana V, Mandin JY, Von der Heyden P, Décatoire D, Plateaux JJ. Oxygen-broadening coefficients of first overtone nitric oxide lines. *JQSRT* 1999;61:759–65.
- [66] Mandin JY, Dana V, Régalia L, Thomas X, Barbe A. Nitrogen-broadening in the nitric oxide first overtone band. *JQSRT* 2000;66:93–100.
- [67] Chackerian Jr C, Freedman RS, Giver LP, Brown LR. The NO vibrational fundamental band: O₂-broadening coefficients. *J Mol Spectrosc* 1998;192:215–9; Spencer MN, Chackerian Jr C, Giver LP, Brown LR. The nitric oxide fundamental band: frequency and shape parameters for ro-vibrational lines. *J Mol Spectrosc* 1994;165:506–24.
- [68] Mandin JY, Dana V, Perrin A, Flaud JM, Camy-Peyret C, Régalia L, Barbe A. The $\{v_1 + 2v_2, v_1 + v_3\}$ bands of ¹⁴N¹⁶O₂: line positions and intensities; line intensities in the $v_1 + v_2 + v_3 - v_2$ hot band. *J Mol Spectrosc* 1997;181:379–88.
- [69] Dana V, Mandin JY, Allout MY, Perrin A, Régalia L, Barbe A, Plateaux JJ, Thomas X. Broadening parameters of NO₂ lines in the 3.4 micron spectral region. *JQSRT* 1997;57:445–57.
- [70] Devi VM, Fridovich B, Jones GD, Snyder DGS, Das PP, Flaud JM, Camy-Peyret C, Rao KN. Tunable diode laser spectroscopy of NO₂ at 6.2 μm. *J Mol Spectrosc* 1982;93:179–95; Devi VM, Fridovich B, Jones GD, Snyder DGS, Neuendorffer A. Temperature dependence of the widths of N₂-broadened lines of the v_3 band of ¹⁴N¹⁶O₂. *Appl Opt* 1982;21:1537–8.
- [71] May RD, Webster CR. Laboratory measurements of NO₂ line parameters near 1600 cm⁻¹ for the interpretation of stratospheric spectra. *Geophys Res Let* 1990;17:2157–60.
- [72] Perrin A, Flaud JM, Camy-Peyret C, Hurtmans D, Herman M, Guelachvili G. The $v_2 + v_3$ and $v_2 + v_3 - v_2$ bands of ¹⁴N¹⁶O₂: line positions and intensities. *J Mol Spectrosc* 1994;168:54–66.
- [73] Kleiner I, Tarrago G, Cottaz C, Sagui L, Brown LR, Poynter RL, Pickett HM, Chen P, Pearson JC, Sams RL, Blake GA, Matsuura S, Nemtchinov V, Varanasi P, Fusina L, Di Lonardo G. NH₃ and PH₃ line parameters: 2000 HITRAN update and new results. *JQSRT*, doi:10.1016/S0022-4073(03)00159-6.
- [74] Goldman A, Rinsland CP, Perrin A, Flaud JM. HNO₃ line parameters: 1996 HITRAN update and new results. *JQSRT* 1998;60:851–61.
- [75] Toth RA, Brown LR, Cohen EA. Line intensities of HNO₃. *J Mol Spectrosc* 2003;218:151–68.
- [76] Flaud JM, Perrin A, Orphal J, Kou Q, Flaud PM, Dutkiewicz Z, Piccolo C. New analysis of the $v_5 + v_9 - v_9$ hot band of HNO₃. *JQSRT* 2003;77:355–64.
- [77] May RD, Webster CR. Measurements of the line positions, intensities, and collisional air-broadening coefficients in the HNO₃ 7.5 – μm band using a computer-controlled tunable diode laser spectrometer. *J Mol Spectrosc* 1989;138:383–97.
- [78] Goldman A, Schoenfeld WG, Goorvitch D, Chackerian C, Dothe H, Mélen F, Abrams MC, Selby JEA. Updated line parameters for OH $X^2\Pi - X^2(v'', v')$ Transitions. *JQSRT* 1998;59:453–69.
- [79] Goldman A, Coffey MT, Hannigan JW, Mankin WG, Chance KV, Rinsland CP. HBr and HI line parameters update for atmospheric spectroscopy databases. *JQSRT*, doi:10.1016/S0022-4073(03)00160-2.
- [80] Fayt A, Vandenhoute R, Lahaye JG. Global rovibrational analysis of carbonyl sulfide. *J Mol Spectrosc* 1986;119:233–66.
- [81] Lahaye JG, Vandenhoute R, Fayt A. CO₂ laser saturation Stark spectra and global Stark analysis of carbonyl sulfide. *J Mol Spectrosc* 1986;119:267–79.
- [82] Masukidi LS, Lahaye JG, Fayt A. Intracavity CO laser Stark spectroscopy of the v_3 band of carbonyl sulfide. *J Mol Spectrosc* 1991;148:281–302.
- [83] Grabow JU, Heineking N, Stahl W. A molecular beam microwave Fourier transform (MB-MWFT) spectrometer with an electric discharge nozzle. *Z Naturforsch* 1991;46A:914–6.
- [84] Maki AG, Wells JS, Burkholder JB. High-resolution measurements of the bands of carbonyl sulfide between 2510 and 3150 cm⁻¹. *J Mol Spectrosc* 1991;147:173–81.
- [85] Horneman VM, Koivusaari M, Tolonen AM, Alanko S, Antilla R, Paso R, Ahonen T. Updating OCS $2v_2$ band for calibration purposes. *J Mol Spectrosc* 1992;155:298–306.
- [86] Masukidi LS, Lahaye JG, Fayt A. Intracavity CO and CO₂ laser Stark spectroscopy of the isotopomers of carbonyl sulfide. *J Mol Spectrosc* 1992;154:137–62.
- [87] Dax A, Mürtz M, Wells JS, Schneider M, Bachem E, Urban W, Maki AG. Extension of heterodyne frequency measurements on OCS to 87 THz (2900 cm⁻¹). *J Mol Spectrosc* 1992;156:98–103.

- [88] George T, Wappelhorst MH, Saupe S, Mürtz M, Urban W, Maki AG. Sub-Doppler heterodyne frequency measurements of carbonyl sulfide transitions between 56 and 62 THz. *J Mol Spectrosc* 1994;167:419–28.
- [89] Dax A, Wells JS, Hollberg L, Maki AG, Urban W. Sub-Doppler frequency measurements on OCS at 87 THz (3.4 μm) with the CO overtone laser. *J Mol Spectrosc* 1994;168:416–28.
- [90] Belafhal A, Fayt A, Guelachvili G. Fourier transform spectroscopy of carbonyl sulfide from 1800 to 3120 cm^{-1} : the normal species. *J Mol Spectrosc* 1995;174:1–19.
- [91] Masukidi LS, Lahaye JG, Belafhal A, Fayt A, Guelachvili G. Infrared spectra of rare isotopic species of OCS. Proceedings of the twelfth colloquium on high resolution molecular spectroscopy, Dijon, September 9–13, 1991; Belafhal A. PhD thesis, Université Catholique de Louvain, 1993.
- [92] Wells JS, Dax A, Hollberg L, Maki AG. Sub-Doppler frequency measurements on OCS near 1689 and 1885 cm^{-1} . *J Mol Spectrosc* 1995;170:75–81.
- [93] Saupe S, Wappelhorst MH, Meyer B, Urban W, Maki AG. Sub-Doppler heterodyne frequency measurements near 5 μm with a CO-laser sideband system: improved calibration tables for carbonyl sulfide transitions. *J Mol Spectrosc* 1996;175:190–7.
- [94] Fichoux H, Rusinek E, Khelkal M, Legrand J, Herlemont F, Fayt A. Saturation sideband CO_2 laser spectroscopy of the overtone band $2\nu_2$ and its hot band $3\nu_2-\nu_2$ of carbonyl sulfide. *J Mol Spectrosc* 1998;189:249–53.
- [95] Hornberger Ch, Boor B, Stuber R, Demtröder W, Naïm S, Fayt A. Sensitive overtone spectroscopy of carbonyl sulfide between 6130 and 6650 cm^{-1} and at 12 000 cm^{-1} . *J Mol Spectrosc* 1996;179:237–45.
- [96] Strugariu T, Naïm S, Fayt A, Bredohl H, Blavier JF, Dubois I. Fourier transform spectroscopy of ^{18}O -enriched carbonyl sulfide from 1825 to 2700 cm^{-1} . *J Mol Spectrosc* 1998;189:206–19.
- [97] Naïm S, Fayt A, Bredohl H, Blavier JF, Dubois I. Fourier transform spectroscopy of carbonyl sulfide from 3700 to 4800 cm^{-1} and selection of a line-pointing program. *J Mol Spectrosc* 1998;192:91–101.
- [98] Rbaihi E, Belafhal A, Vander Auwera J, Naïm S, Fayt A. Fourier transform spectroscopy of carbonyl sulfide from 4800 to 8000 cm^{-1} and new global analysis of $^{16}\text{O}^{12}\text{C}^{32}\text{S}$. *J Mol Spectrosc* 1998;191:32–44.
- [99] Mürtz M, Palm P, Urban W, Maki AG. More sub-Doppler heterodyne frequency measurements on OCS between 56 and 63 THz. *J Mol Spectrosc* 2000;204:281–5.
- [100] Kagann RH. Infrared absorption intensities for OCS. *J Mol Spectrosc* 1982;94:192–8.
- [101] Dang-Nhu M, Guelachvili G. Intensités des raies d'absorption dans la bande $\nu_2 + \nu_3$ de $^{16}\text{O}^{12}\text{C}^{32}\text{S}$. *Mol Phys* 1986;58:535–40.
- [102] Bouanich JP, Blanquet G, Walrand J, Courtoy CP. Diode laser measurements of line strengths and collisional half-widths in the ν_1 band of OCS at 298 and 200 K. *JQSRT* 1986;36:295–306.
- [103] Blanquet G, Coupe P, Derie F, Walrand J. Spectral intensities in the $2\nu_2^0$ band of carbonyl sulfide. *J Mol Spectrosc* 1991;147:543–5.
- [104] Errera Q, Vander Auwera J, Belafhal A, Fayt A. Absolute intensities in $^{16}\text{O}^{12}\text{C}^{32}\text{S}$: the 2500–3100 cm^{-1} region. *J Mol Spectrosc* 1995;173:347–69.
- [105] Brown LR. Private communication.
- [106] Régalia-Jarlot L, Hamdouni A, Thomas X, Von der Heyden P, Barbe A. Line intensities of the: ν_3 , $4\nu_2$, $\nu_1 + \nu_3$, $3\nu_1$, and $2\nu_1 + \nu_2$ bands of the $^{16}\text{O}^{12}\text{C}^{32}\text{S}$ molecule. *JQSRT* 2002;74:455–70.
- [107] Bermejo D, Domenech JL, Santos J, Bouanich JP, Blanquet G. Absolute line intensities in the $2\nu_3$ band of $^{16}\text{O}^{12}\text{C}^{32}\text{S}$. *J Mol Spectrosc* 1997;185:26–30.
- [108] Mouchet A, Blanquet G, Herbin P, Walrand J, Courtoy CP. Diode laser measurements of N_2 -broadened linewidths in the ν_1 band of OCS. *Can J Phys* 1985;63:527–31.
- [109] Bouanich JP, Walrand J, Albery S, Blanquet G. Diode laser measurements of oxygen-broadened linewidths in the ν_1 band of OCS. *J Mol Spectrosc* 1987;123:37–47.
- [110] Bouanich JP, Blanquet G. Pressure broadening of CO and OCS spectral lines. *JQSRT* 1988;40:205–20.
- [111] Domenech JL, Bermejo D, Bouanich JP. Pressure lineshift and broadening coefficients in the $2\nu_3$ band of $^{16}\text{O}^{12}\text{C}^{32}\text{S}$. *J Mol Spectrosc* 2000;200:266–76.
- [112] Flaud JM, Birk M, Wagner G, Orphal J, Klee S, Lafferty WJ. The far-infrared spectrum of HOCl: line positions and intensities. *J Mol Spectrosc* 1998;191:362–7.
- [113] Vander Auwera J, Kleffmann J, Flaud JM, Pawelke G, Burger H, Hurtmans D, Petrisse R. Absolute ν_2 line intensities of HOCl by simultaneous measurements in the infrared with a tunable diode laser and far-infrared region using a Fourier transform spectrometer. *J Mol Spectrosc* 2000;204:36–47.

- [114] Maki AG, Mellau GC, Klee S, Winnewisser M, Quapp W. High-temperature infrared measurements in the region of the bending fundamental of $\text{H}^{12}\text{C}^{14}\text{N}$, $\text{H}^{12}\text{C}^{15}\text{N}$, and $\text{H}^{13}\text{C}^{14}\text{N}$. *J Mol Spectrosc* 2000;202:67–82.
- [115] Maki AG, Quapp W, Klee S, Mellau GC, Albert S. Infrared Transitions of $\text{H}^{12}\text{C}^{14}\text{N}$ and $\text{H}^{12}\text{C}^{15}\text{N}$ between 500 and 10 000 cm^{-1} . *J Mol Spectrosc* 1996;180:323–36.
- [116] Devi VM, Benner DC, Smith MAH, Rinsland CP, Sharpe SW, Sams RL. A multispectrum analysis of the ν_1 band of $\text{H}^{12}\text{C}^{14}\text{N}$: I. Intensities, self-broadening and self-shift coefficients. *JQSRT*, doi:10.1016/S0022-4073(03)00161-4.
- [117] Rinsland CP, Devi VM, Smith MAH, Benner DC, Sharpe SW, Sams RL. A multispectrum analysis of the ν_1 band of $\text{H}^{12}\text{C}^{14}\text{N}$: II. Air- and N_2 -broadening, shifts and their temperature dependences. *JQSRT*, doi:10.1016/S0022-4073(03)00162-6.
- [118] Chackerian Jr C, Brown LR, Lacombe N, Tarrago G. Methyl chloride ν_5 region line shape parameters and rotational constants for the ν_2 , ν_5 and $2\nu_3$ vibrational bands. *J Mol Spectrosc* 1998;191:148–57.
- [119] Perrin A, Flaud JM, Camy-Peyret C, Schermaul R, Winnewisser M, Mandin JY, Dana V, Badaoui M, Koput J. Line intensities in the far-infrared spectrum of H_2O_2 . *J Mol Spectrosc* 1996;176:287–96.
- [120] Klee S, Winnewisser M, Perrin A, Flaud JM. Absolute line intensities for the ν_6 band of H_2O_2 . *J Mol Spectrosc* 1999;195:154–61.
- [121] Rinsland CP, Jones NB, Connor BJ, Logan JA, Pougatchev NS, Goldman A, Murcray FJ, Stephen TM, Pine AS, Zander R, Mahieu E, Demoulin P. Northern and southern hemisphere ground-based infrared spectroscopic measurements of tropospheric carbon monoxide and ethane. *J Geophys Res* 1998;103:28,197–217.
- [122] Brown LR. Private communication, 2001.
- [123] Brown LR, Crisp JA, Crisp D, Naumenko OV, Smirnov MA, Sinitisa LN, Perrin A. The absorption spectrum of H_2S between 2150 and 4260 cm^{-1} : analysis of the positions and intensities in the first [$2\nu_2$, ν_1 and ν_3] and second [$3\nu_2$, $\nu_1 + \nu_2$ and $\nu_2 + \nu_3$] triad region. *J Mol Spectrosc* 1998;188:148–74.
- [124] Sumpf B. Private communication, 2000.
- [125] Kissel A, Sumpf B, Kronfeldt HD, Tikhomirov BA, Ponomarev YN. Molecular-gas-pressure-induced line-shift and line-broadening in the ν_2 -band of H_2S . *J Mol Spectrosc* 2002;216:345–54.
- [126] Perrin A, Rinsland CP, Goldman A. Spectral parameters for the ν_6 region of HCOOH and its measurement in the infrared tropospheric spectrum. *J Geophys Res* 1999;104:18,661–6.
- [127] Chance KV, Park K, Evenson KM, Zink LR, Stroth F, Fink EH, Ramsay DA. Improved molecular constants for the ground state of HO_2 . *J Mol Spectrosc* 1997;183:418.
- [128] Saito S, Matsumura C. Dipole moment of the HO_2 radical from its microwave spectrum. *J Mol Spectrosc* 1980;80:34–40.
- [129] Nelson DD, Zahniser MS. Air broadening measurements for the ν_2 vibrational band of the hydroperoxyl radical. *J Mol Spectrosc* 1994;166:273–9.
- [130] Cauuet I, Walrand J, Blanquet G, Valentin A, Henry L, Lambeau Ch, DeVleeschouwer M, Fayt A. Extension to third-order Coriolis terms of the analysis of ν_{10} , ν_7 , and ν_4 levels of ethylene on the basis of Fourier transform and diode laser spectra. *J Mol Spectrosc* 1990;139:191–214.
- [131] Legrand J, Azizi M, Herlemont F, Fayt A. Saturation spectroscopy of C_2H_4 using a CO_2 laser sideband spectrometer. *J Mol Spectrosc* 1995;171:13–21.
- [132] Rusinek E, Fichoux H, Khelkhal M, Herlemont F, Legrand J, Fayt A. Sub-Doppler study of the ν_7 band of C_2H_4 with a CO_2 laser side band spectrometer. *J Mol Spectrosc* 1998;189:64–73.
- [133] Pine AS. Tunable laser survey of molecular air pollutants. Final Report NSF/ASRA/DAR 78-24562, MIT, Lexington, MA, 1980.
- [134] Blass WE, Jennings L, Ewing AC, Daunt SJ, Weber MC, Senesac L, Hager S, Hillman JJ, Reuter DC, Sirota JM. Absolute intensities in the ν_7 band of ethylene: tunable laser measurements used to calibrate FTS broadband spectra. *JQSRT* 2001;68:467–72.
- [135] Dang-Nhu M, Pine AS, Fayt A, DeVleeschouwer M, Lambeau C. Les intensités dans la pentade ν_{11} , $\nu_2 + \nu_{12}$, $2\nu_{10} + \nu_{12}$, ν_9 et $\nu_3 + \nu_8 + \nu_{10}$ de $^{12}\text{C}_2\text{H}_4$. *Can J Phys* 1983;61:514–21.
- [136] Brannon JF, Varanasi P. A tunable diode laser measurements on the 951.7393 cm^{-1} Line of $^{12}\text{C}_2\text{H}_4$ at planetary atmospheric temperatures. *JQSRT* 1992;47:237–42.
- [137] Varanasi P, Nemtchinov V, Li Z, Cherukuri A. Spectral absorption-coefficient data on HCFC-22 and SF_6 for remote sensing applications. *JQSRT* 1994;52:323–32.
- [138] Varanasi P. Private communication, 2000.

- [139] Birk M, Wagner G. A new spectroscopic database for chlorine nitrate. Poster 30, Sixth Biennial HITRAN Conference, Cambridge, MA, USA, 19–21 June, 2000.
- [140] Ballard J, Johnston WB, Gunson MR, Wassell PT. Absolute absorption coefficients of ClONO₂ infrared bands at stratospheric temperatures. *J Geophys Res* 1988;93:1659–65.
- [141] Nemtchinov V, Varanasi P. Thermal infrared absorption cross-sections of CCl₄ needed for atmospheric remote-sensing. *JQSRT*, doi:10.1016/S0022-4073(03)00171-7.
- [142] Massie ST, Goldman A, Murcray DG, Gille JC. Approximate absorption cross sections of F12, F11, ClONO₂, N₂O₅, HNO₃, CCl₄, CF₄, F21, F113, F114, and HNO₄. *Appl Opt* 1985;24:3426–7.
- [143] Zou Q, Sun C, Nemtchinov V, Varanasi P. Thermal infrared cross-sections of C₂F₆ at atmospheric temperatures. *JQSRT*, 2003, doi:10.1016/S0022-4073(02)00353-9.
- [144] Varanasi P, Nemtchinov V. Thermal infrared absorption coefficients of CFC-12 at atmospheric conditions. *JQSRT* 1994;51:679–87.
- [145] McDaniel AH, Cantrell CA, Davidson JA, Shetter RE, Calvert JG. The temperature dependent, infrared absorption cross sections for the chlorofluorocarbons: CFC-11, CFC-12, CFC-13, CFC-14, CFC-22, CFC-113, CFC-114, and CFC-115. *J Atmos Chem* 1991;12:211–27;
Massie ST, Goldman A, McDaniel AH, Cantrell CA, Davidson JA, Shetter RE, Calvert JG. Temperature dependent infrared cross sections for CFC-11, CFC-12, CFC-13, CFC-14, CFC-22, CFC-113, CFC-114, and CFC-115. NCAR Technical Note/TN-358+STR, 1991.
- [146] Nemtchinov V, Varanasi P. Thermal infrared absorption cross-sections of CF₄ for atmospheric applications. *JQSRT*, doi:10.1016/S0022-4073(03)00170-5.
- [147] Clerbaux C, Colin R, Simon PC, Granier C. Infrared cross sections and global warming potentials of 10 alternative hydrohalocarbons. *J Geophys Res* 1993;98:10,491–7.
- [148] Smith K, Newnham D, Page M, Ballard J, Duxbury G. Infrared band strengths and absorption cross-sections of HFC-32 vapour. *JQSRT* 1996;56:73–82.
- [149] Smith K, Newnham D, Page M, Ballard J, Duxbury G. Infrared absorption cross-sections and integrated absorption intensities of HFC-134 and HFC-143a vapour. *JQSRT* 1998;59:437–51.
- [150] Nemtchinov V, Varanasi P. Absorption cross-sections of HFC-134a in the spectral region between 7 and 12 μm. *JQSRT* 2003, doi:10.1016/S0022-4073(02)00356-4.
- [151] Varanasi P. Absorption spectra of HCFC-22 around 829 cm⁻¹ at atmospheric conditions. *JQSRT* 1992;47:251–5.
- [152] Zander R, Rinsland CP, Farmer CB, Norton RH. Infrared spectroscopic measurements of halogenated source gases in the stratosphere with the ATMOS instrument. *J Geophys Res* 1987;92:9836–50.
- [153] Hartmann J-M, Kochel J-M, Payan S, Camy-Peyret C, Engel A. CCl₂F₂ mixing ratio profiles in the 1995 late winter arctic vortex from balloon-borne spectra. *Geophys Res Lett* 1997;24(19):2367–70.
- [154] Coheur PF, Clerbaux C, Colin R. Spectroscopic measurements of halocarbons and hydrohalocarbons by satellite-borne remote sensors. *J Geophys Res* 2003;108:ACH 1-1–ACH 1-14.
- [155] Ballard J, Knight RJ, Newnham DA, Vander Auwera J, Herman M, Di Lonardo G, Masciarelli G, Nicolaisen FM, Beukes JA, Christensen LK, McPheat R, Duxbury G, Freckleton R, Shine KP. An intercomparison of laboratory measurements of absorption cross sections and integrated absorption intensities for HCFC-22. *JQSRT* 2000;66: 109–28.
- [156] Gillis JR, Goldman A, Stark G, Rinsland CP. Line parameters for the $A^2\Sigma^+ - X^2\Pi$ bands of OH. *JQSRT* 2000;68: 225–30.
- [157] Vandaele AC, Hermans C, Simon PC, Carleer M, Colin R, Fally S, Mérienne MF, Jenouvrier A, Coquart B. Measurements of the NO₂ absorption cross-section from 42 000 cm⁻¹ to 10 000 cm⁻¹ (238–1000 nm) at 220 K and 294 K. *JQSRT* 1997;59:171–84.
- [158] Bohren CF, Huffman DR. Absorption and scattering of light by small particles. New York: Wiley-Interscience, 1983. p. 71–2.
- [159] Thomas GE, Stamnes K. Radiative transfer in the atmosphere and ocean. Cambridge: Cambridge University Press, 1999. p. 174.
- [160] Massie ST, Goldman A. HITRAN 2000 infrared cross sections and indices of refraction. *JQSRT*, doi:10.1016/S0022-4073(03)00167-5.
- [161] Toon OB, Tolbert MA, Koehler BG, Middlebrook AE, Jordan J. Infrared optical constants of H₂O ice, amorphous nitric acid solutions, and nitric acid hydrates. *J Geophys Res* 1994;99:25,631–54.

- [162] Richwine LJ, Clapp ML, Miller RE, Worsnop DR. Complex refractive indices in the infrared of nitric acid trihydrate aerosols. *Geophys Res Lett* 1995;22:2625–8.
- [163] Massie ST. Indices of refraction for the HITRAN compilation. *JQSRT* 1994;52:501–13.
- [164] Tisdale RT, Glandorf DL, Tolbert MA, Toon OB. Infrared optical constants of low-temperature H₂SO₄ solutions representative of stratospheric sulfate aerosols. *J Geophys Res* 1998;103:25,353–70.
- [165] Niedziela RF, Norman ML, deForest CI, Miller RE, Worsnop DR. A temperature and composition-dependent study of H₂SO₄ aerosol optical constants using Fourier transform and tunable diode laser infrared spectroscopy. *J Phys Chem A* 1999;103:8030–40.
- [166] Biermann UM, Luo BP, Peter Th. Absorption spectra and optical constants of binary ternary solutions of H₂SO₄, HNO₃, and H₂O in the mid infrared at atmospheric temperatures. *J Phys Chem A* 2000;104:783–93.
- [167] Norman ML, Qian J, Miller RE, Worsnop DR. Infrared complex refractive indices of supercooled liquid HNO₃/H₂O aerosols. *J Geophys Res* 1999;104:30,571–84.
- [168] Palmer KF, Williams D. Optical constants of sulfuric acid; application to the clouds of Venus? *Appl Opt* 1975;14:208–19.
- [169] Pickett HM, Poynter RL, Cohen EA, Delitsky ML, Pearson JC, Müller HSP. Submillimeter, millimeter, and microwave spectral line catalogue. *JQSRT* 1998;60:883–90.
- [170] Fischer J, Gamache RR, Goldman A, Rothman LS, Perrin A. Total internal partition sums for molecular species on the 2000 edition of the HITRAN database. *JQSRT*, doi:10.1016/S0022-4073(03)00166-3.